Organic Thin Film Transistors for Large Area Electronics

By *Christos D. Dimitrakopoulos** and *Patrick R. L. Malenfant*

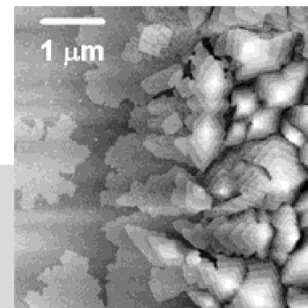

Organic thin-film transistors (OTFTs) have lived to see great improvements in recent years. This review presents new insight into conduction mechanisms and performance characteristics, as well as opportunities for modeling properties of OTFTs. The shifted focus in research from novel chemical structures to fabrication technologies that optimize morphology and structural order is underscored by chapters on vacuum-deposited and solution-processed organic semiconducting films. Finally, progress in the growing field of the n-type OTFTs is discussed in ample detail. The Figure, showing a pentacene film edge on SiO_2, illustrates the morphology issue.

1. Introduction

Organic semiconductors have been studied since the late 1940s.[1] However, until recently they had failed to have a significant practical impact in optoelectronic applications, despite of the fact that a very large number of experimental and theoretical studies have been published. Initial industrial applications of organic semiconductors exploited their photoconductive properties in xerography. The initial demonstration of organic electroluminescent diodes[2,3] and OTFTs[4–6] based on either small organic molecules[2,5] or conjugated polymers,[3,4,6] and the impressive improvements in performance, and efficiency of organic devices during the last decade[7–10] attracted the interest of industry and opened the way to practical applications for organic semiconductors. In this review we will focus on the progress in the field of OTFTs in recent years. We will restrict our review to transistors in which the organic active layer is an approximately two-dimensional structure, such as a thin film. It has been shown that only a few organic monolayers are sufficient for proper transistor operation.[11,12] We will make an effort to describe the broad spectrum of materials, fabrication processes, designs, and applications of OTFTs, with an emphasis on papers published during the last few years. Older papers that, in the authors' opinion, played a pivotal role in shaping the OTFT field are also reviewed, but the reader is encouraged to look up a number of previously published review papers that cover that earlier period in more detail.[13–19] Reported results from single crystal organic field effect transistors will be used to define the upper limit of performance of OTFTs and to gain a better understanding of the underlying device physics. Results from devices in which the active channel consists of a single organic molecule or a more extended structure such as a carbon nanotube, will not be discussed, despite the strong interest that recently has developed for such transistors.[20–24]

As in traditional inorganic semiconductors, organic materials can function either as p-type or n-type. In p-type semiconductors the majority carriers are holes, while in n-type the majority carriers are electrons. The most widely studied organic semiconductors have been p-type, however, due to the recent appearance of several new reports on OTFTs based on n-type organic semiconductors, we have devoted a separate section of this review to n-type organics. Pentacene, one of the most widely studied organic semiconductors for OTFTs, is used to demonstrate many of the physical phenomena discussed in this review, due to its superior field effect mobility and environmental stability, although a broad spectrum of organic semiconducting materials is also covered.

OTFTs based on conjugated polymers, oligomers, or fused aromatics have been envisioned as a viable alternative to more traditional, mainstream thin film transistors (TFTs) based on inorganic materials. Because of the relatively low mobility of organic semiconductors, OTFTs cannot rival the performance of field-effect transistors based on single-crystalline inorganic semiconductors, such as Si, Ge, and GaAs, which have charge carrier mobilities (μ) of three or more orders of magnitude higher.[25] Consequently, OTFTs are not suitable for use in applications requiring very high switching

[*] Dr. C. D. Dimitrakopoulos, Dr. P. R. L. Malenfant[+]
IBM Corporation, T. J. Watson Research Center
P.O. Box 218, Yorktown Heights, NY 10598 (USA)
E-mail: dimitrak@us.ibm.com

[+] Present address: GE CRD, Emerging Technologies, K1-4A49, 1 Research Circle, Niskayuna, NY 12309, USA.

 © WILEY-VCH Verlag GmbH, D-69469 Weinheim, 2002 0935-9648/02/0201-0099 $ 17.50+.50/0

speeds. However, the unique processing characteristics and demonstrated performance of OTFTs suggest that they can be competitive candidates for existing or novel thin film transistor applications requiring large area coverage, structural flexibility, low temperature processing, and especially low cost. Such applications include switching devices for active matrix flat panel displays (AMFPDs) based on liquid crystal pixels (AMLCDs), organic light emitting diodes (AMOLEDDs), or "electronic paper" displays[26] based on pixels comprising either electrophoretic ink-containing microcapsules[27] or "twisting balls".[28] Additionally, sensors,[29] low-end smart cards, and radio-frequency identification tags (RFIDs) consisting of organic integrated circuits have been proposed and prototype all-polymer integrated circuits have been demonstrated.[30]

Different applications will require different performance standards. At present, the entrenched technology in large area electronics applications, especially backplanes of AMLCDs, is based on TFTs comprising hydrogenated amorphous silicon (a-Si:H) active layers. However, OTFTs can enable applications that are not achievable using the entrenched technology, taking advantage of the fact that OTFTs, can be processed at or close to room temperature (RT) and thus are compatible with transparent plastic substrates. Because of the high processing temperature used during a-Si:H deposition (ca. 360 °C), it is not possible to make an AMLCD based on such TFTs on a transparent plastic substrate. For OTFTs to compete directly with a-Si:H TFTs, the former should exhibit device performance similar to that of the latter, i.e., field effect mobility $\mu = 1\ cm^2\,V^{-1}\,s^{-1}$, and current modulation (or on/off ratio, $I_{on/off}$) of 10^6 or higher at a maximum operating voltage of about 15 V or less. Additionally, they should be stable after prolonged exposure to ambient conditions, and should not exhibit large threshold voltage shifts.

2. Progress in Performance of p-Type Organic Thin-Film Field-Effect Transistors from 1984 to the Present Time

In a previous paper[7a] we presented a semi-logarithmic plot of each year's highest reported field-effect mobility value from TFTs based on various organic semiconductors since 1986. An updated and more complete version of that plot, based on Table 1 that includes results from p-type organic semiconductors only, is shown in Figure 1.

Table 1 lists the highest field-effect mobility (μ) values measured from p-type OTFTs as reported in the literature, annually from 1984 to the present time, for each one of the most promising p-type organic semiconductors. For a specific p-type organic semiconductor that already has an entry in Table 1 and Figure 1 for a previous year, a new mobility value is entered only if it is higher than the value of the preceding entry. We can observe an impressive increase in mobility, which came about either by improving the processes used for the fabrication of the transistors or by synthesizing new organic materials. A typical path to performance increase could be described as a three-stage process: a) A new organic semicon-

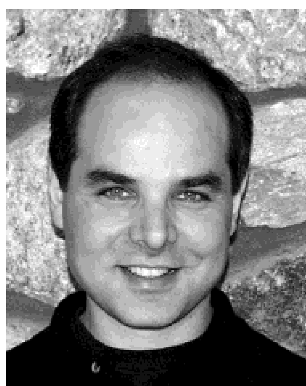

Dr. Christos Dimitrakopoulos is a Research Staff Member at IBM, T. J. Watson Research Center, Yorktown Heights, NY, USA, where he works on organic semiconductor devices and circuits. He has been with IBM since 1995. From 1993 to 1995 he was a post-doctoral fellow at Philips Research Laboratories in Eindhoven, The Netherlands, where he also worked on organic semiconductors. He holds Ph.D., M.Phil., and M.Sc. degrees in Materials Science from Columbia University. He also holds a B.Sc. Degree in Metallurgical Engineering from the National Technical University of Athens, Greece. He is the author or co-author of four patents, seven pending patents and at least 20 papers. He has received an IBM Outstanding Innovation Award, for "High Performance Organic Transistors on Plastic".

Dr. Patrick Roland Lucien Malenfant was born in 1971 in Kapuskasing, Ontario and was raised in Timmins, Ontario, Canada until he attended college. He obtained his B.Sc. Honours co-op degree in Chemistry from the University of Ottawa in 1995. He received a M.S. from Cornell University in 1997 and a Ph.D. degree from the University of California at Berkeley in 2000 with Jean M. J. Fréchet. The main focus of his thesis was the synthesis of well-defined conjugated oligothiophenes and their combination with dendrimers. New synthetic methods were also devised that led to the first solid-phase synthesis of oligothiophenes. After graduation, he took a post-doctoral position at IBM's T. J. Watson Research Center in Yorktown Heights, NY where he worked in the area of organic electronics. He is currently working at GE Corporate Research and Development (CRD) in Niskayuna, NY as a member of the Emerging Technologies group.

 © WILEY-VCH Verlag GmbH, D-69469 Weinheim, 2002 0935-9648/02/0201-0100 $ 17.50+.50/0

Table 1. The highest field-effect mobility (μ) values measured from p-type OTFTs as reported in the literature, annually from 1984 to the present time, for each one of the most promising p-type organic semiconductors.

Year	Mobility [a] [$cm^2 V^{-1} s^{-1}$]	Material (deposition method) [b]	I_{on}/I_{off} [c]	W/L	Reference
1964	NR [d]	Cu-phthalocyanine (v) (first demonstration of field effect in small organic molecules)	NR	NR	[140]
1983	NR	Polyacetylene (s) (first demonstration of field effect in polymers)	NR	200	[4]
1984	1.5×10^{-5}	Merocyanine	NR	7000	[5]
1986	10^{-5}	Polythiophene (s)	10^3	NR	[6]
1988	10^{-4}	Polyacetylene (s)		750	[113]
	10^{-3}	Phthalocyanine (v)	NR	3	[141]
	10^{4}	Poly(3-hexylthiophene) (s)	NR	NR	[85]
1989	10^{-3}	Poly(3-alkylthiophene) (s)	NR	NR	[142]
	10^{-3}	α-sexithiophene (v)	NR	NR	[65]
1992	0.027	α-sexithiophene (v)	NR	100	[66]
	2×10^{-3}	Pentacene (v)	NR	NR	[66]
1993	0.05	α-ω-dihexyl-sexithiophene (v)	NR	100-200	[67]
	0.22 [e]	Polythienylenevinylene (s)	NR	1000	[143]
1994	0.06	α-ω-dihexyl-sexithiophene (v)	NR	50	[144]
1995	0.03	α-sexithiophene (v)	$>10^6$	21	[12]
	0.038	Pentacene (v)	140	1000	[50]
1996	0.02	Phthalocyanine (v)	2×10^5	NR	[145]
	0.045	Poly(3-hexylthiophene) (s)	340	20.8	[89]
	0.62	Pentacene (v)	10^8	11	[59]
1997	1.5	Pentacene (v)	10^8	2.5	[38]
	0.13	α-ω-dihexyl-sexithiophene (v)	$>10^4$	7.3	[7a]
	0.05	Bis(dithienothiophene) (v)	10^8	500	[146]
1998	0.1	Poly(3-hexylthiophene) (s)	$>10^6$	20	[91]
	0.23	α-ω-dihexyl-quaterthiophene (v)	NR	1.5	[147]
	0.15	Dihexyl-anthradithiophene	NR	1.5	[108]
2000	0.1	α-ω-dihexyl-quinquethiophene (s)	NR	NR	[105]
	2.4	pentacene (v)	10^8	10-100	[31]

[a] Measured at RT. [b] (v) = vacuum deposition, (s) = from solution. [c] Values for I_{on}/I_{off} correspond to different gate voltage ranges and thus are not readily comparable to each other. The reader is encouraged to read the details of the experiments in the cited references. [d] NR = not reported. [e] This result has not yet been reproduced.

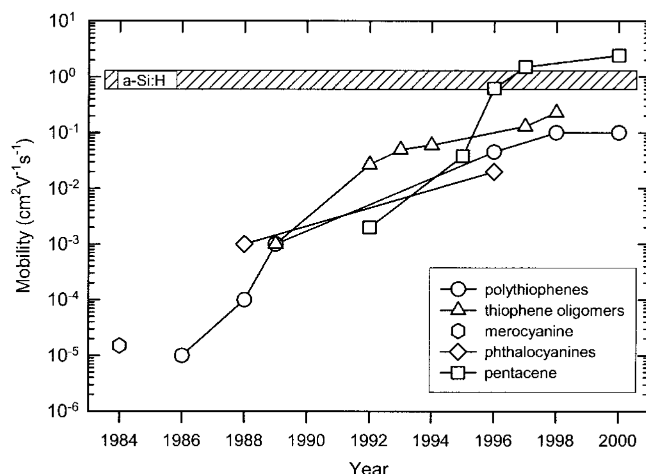

Fig. 1. Evolution of OTFT hole mobility for the most common p-type organic semiconductors. The various p-type materials are grouped together into families of similar molecules taking into account only the core part of each molecule. For reference, a representative range of electron mobilities for a-Si:H TFT is shown. The hole mobility in a-Si:H TFT is much lower than the electron mobility.

ductor is synthesized or a known one is used for the first time as the active layer in an OTFT. b) The film deposition parameters for the semiconducting organic layer are optimized to obtain the most advantageous structural and morphological characteristics for improved performance until no more improvement seems possible. c) The source and drain contacts and the general transistor configuration are optimized. After this point, another incremental improvement in mobility is usually obtained from the synthesis and/or first OTFT application of a new organic semiconductor. Today, we have reached an important point in the performance versus time plot. The most widely used organic semiconductors, such as pentacene, thiophene oligomers, and regioregular poly(3-alkyl-thiophene), seem to have reached "maturity" as far as their performance is concerned. Their individual performance versus time curves seem to have saturated (re: when a new, higher value is not reported in the years following the last entry for a material, it means that there was no improvement in mobility during those years). In the past, each time such a performance saturation occurred (Fig. 1), a new material was introduced whose performance broke the temporarily established upper limit in performance.

For instance, one can argue that today's maximum hole field effect mobility of 2.4 $cm^2 V^{-1} s^{-1}$ for OTFT (pentacene, measured at RT)[31] has approached a fundamental limit, at least as far as the known classes of semiconducting organic materials are concerned. This pentacene thin film was grown from the vapor phase in a stream of flowing gas (hydrogen or forming gas), in an apparatus similar to the one described in the literature[32–35] and its grain size exceeded the channel length (L) of the TFTs used to determine the field effect mobility. Consequently, this value is very close to RT field effect mobility values of 3.2 and 2.7 $cm^2 V^{-1} s^{-1}$ reported by Schön et al.,[31,36] for holes in pentacene single crystals grown from the vapor phase under hydrogen or forming gas flow, while the substrate was held at relatively high temperature.[34,35] In the following section we will discuss the potential existence of a fundamental limit for charge carrier mobility in conjunction with the various conduction mechanisms believed to be in operation in various organic semiconductors.

3. Conduction Mechanisms in Organic Semiconductors

The upper limit of microscopic mobilities in organic molecular crystals, determined at 300 K by time-of-flight (TOF) experiments, falls between 1 and 10 $cm^2 V^{-1} s^{-1}$.[1] The weak intermolecular interaction forces in organic semiconductors, typically van der Waals interactions with energies smaller than 10 kcal mol^{-1}, may be responsible for this limit, since the vibrational energy of the molecules reaches a magnitude close to that of the intermolecular "bonding" energies at or above RT. In contrast, in inorganic semiconductors such as Si, Ge, and GaAs, the atoms are held together with very strong covalent bonds, which in the case of Si have energies as high as 76 kcal mol^{-1}. In these semiconductors, charge carriers move as highly delocalized plane waves in wide bands and have a very high mobility at RT ($\mu \sim 10^3$ $cm^2 V^{-1} s^{-1}$). In this case, the

 © WILEY-VCH Verlag GmbH, D-69469 Weinheim, 2002 0935-9648/02/0201-0101 $ 17.50+.50/0

mobility is limited by lattice vibrations (phonons) that scatter the carriers and thus it is reduced as the temperature increases.

Band transport is not applicable to disordered organic semiconductors, where carrier transport takes place by hopping between localized states and carriers are scattered at every step. Hopping is assisted by phonons and the mobility increases with temperature, although typically it remains very low overall ($\mu \ll 1$ cm^2 V^{-1} s^{-1}). The boundary between band transport and hopping is defined by materials having RT mobilities of the order of 1 cm^2 V^{-1} s^{-1}.[1,18,37] Thin films of highly ordered organic semiconductors, such as several members of the acene series including pentacene, have RT mobilities in this intermediate range.[37–39] In some cases temperature independent mobility has been observed,[1] even in polycrystalline thin films of pentacene.[37] This observation was used to argue that a simple thermally activated hopping mechanism can be excluded as a transport mechanism in high-quality polycrystalline thin films of pentacene despite of the fact that in some samples containing a large concentration of traps related to structural defects and chemical impurities the mobility increases with temperature.[37] Trapping at the grain boundaries in polycrystalline films of pentacene and the dependence of trap concentration on the film deposition conditions has been suggested as the main cause of the observed variability of the temperature dependence of mobility.[31]

Understanding the transport mechanism in single crystals of organic semiconductors will facilitate our understanding of transport in the technologically more relevant polycrystalline thin films of these materials. At low temperatures, coherent band-like transport of delocalized carriers becomes the prevalent transport mechanism in single crystals of pentacene, tetracene, and other acenes. Very high mobility values have been measured using TOF experiments (up to 400 cm^2 V^{-1} s^{-1} for holes in single crystals of naphthalene at 4.2 K)[40,41] and field effect experiments (up to ~10^5 cm^2 V^{-1} s^{-1} for holes in single crystals of tetracene and pentacene at 1.7 K).[31,42] In the latter experiments, the mobility increases from its RT value of approximately 3 cm^2 V^{-1} s^{-1} to about 10^5 cm^2 V^{-1} s^{-1} at 1.7 K following a power law ($\mu \propto T^{-n}$, $n = 2.7$),[36,42,43] in agreement with earlier work in which $n = 2.9$ was reported.[41,44] At 1.7 K an effective electronic bandwidth of ~0.5 eV ($\gg k_B T$, where k_B is the Boltzmann constant) is estimated from the low effective mass for holes, measured to be of the order of 1 to 1.5m_e, where m_e is the free electron mass.[42] Furthermore, both the integer and fractional quantum Hall effects were observed in acene single crystals.[42] All this is clear evidence of band transport, at low temperatures, in such crystals. In 1974, Burland observed cyclotron resonance of holes in high quality single crystals of anthracene at 2 K, the first time such an observation was made in a wide band gap molecular crystal.[45,46] From the reported values of the effective mass of holes, m^*, in these crystals, determined to be 11m_e, where m_e is the free electron mass, and the hole scattering time, τ, measured to be ~7×10^{-11} and 4×10^{-10} s, respectively in two different anthracene crystals, one could calculate hole mobility values of about 11 200 and 64 000 cm^2 V^{-1} s^{-1}, using the formula: $\mu = (e\, m^{*-1})\tau$, where e is the elementary charge. This was the first time that evidence of such enormously high charge carrier mobility values in organic semiconductors was presented.[45] The temperature dependence of the electron mobility in pentacene and tetracene single crystals was shown to follow the same power law that describes the hole mobility temperature dependence in the same materials, from 1.7 to 300 K. From all the work presented above, it is apparent that extremely high quality, ultra pure single crystals of organic semiconductors are required to obtain such high mobilities and observe the described phenomena. This behavior is rather impossible to observe in polycrystalline films when transport through two or more grains is studied, because traps attributed to grain boundaries and other structural defects dominate transport. Experiments that study electrical transport through only one individual crystallite (grain), which is part of a polycrystalline film, are considered here to be studies of electrical transport in organic semiconductor single crystals.

The temperature dependence of the electron mobility in naphthalene single crystals below 100 K also follows a power law along all three principal directions in the crystal, although with a lower exponent ($\mu \propto T^{-n}$, $n \approx 1.5$ to 1.7), consistent with the band model.[40,44,47] However, between 100 K and 300 K the electron mobility along the c crystallographic direction remains practically constant.[44,47,48] The $\mu(T)$ = constant region has been described phenomenologically as the superposition of two independent carrier mechanisms. According to one interpretation the first mechanism is described using the concept of an adiabatic, nearly small molecular polaron (MP),[47] which is an alternative way to rationalize the power law dependence alongside the delocalized band transport model. According to this model the carriers are treated as heavy polaron-type quasiparticles, which are formed as a result of the interaction of the carriers with intramolecular vibrations of the local lattice environment, and move coherently via tunneling. In this model the mobility follows the power law $\mu_{MP} = aT^{-n}$.[47] The second mechanism involves a small lattice polaron (LP), which moves by thermally activated hopping and thus exhibits a typical exponential dependence of mobility on temperature: $\mu_{LP} = b\exp[-E_a/kT]$. The superposition of these two mechanisms can reproduce the experimentally measured temperature dependence of mobility from just a few degrees K to RT.[47]

Band-like transport of delocalized carriers is also shown to be the prevalent transport mechanism along the crystal directions with high π–π^* orbital overlap, in single crystals of α-sexithiophene (6T) and α-quaterthiophene (4T).[43]

In the following sections we will discuss carrier transport in various polycrystalline thin films of organic semiconductors, assuming that transport in individual crystallites in the film takes place according to the mechanisms described in this section.

At this point we can propose two possible ways for eliminating the potential fundamental upper limit of about 10 cm^2 V^{-1} s^{-1} for the RT mobility of OTFTs, imposed by the

 © WILEY-VCH Verlag GmbH, D-69469 Weinheim, 2002 0935-9648/02/0201-0102 $ 17.50+.50/0

weak intermolecular forces existing among nearest-neighbor (nn) molecules. One is to strengthen such interactions. This can be done by creating a stronger bond between nn molecules. However, this has to take place without breaking the conjugation of the molecules, and without reducing the intermolecular overlap between nn molecules. Stronger intermolecular interactions would result in more rigid crystalline structures, and thus it would take temperatures higher than RT to generate substantial scattering of highly delocalized carriers by lattice vibrations. Using such a strategy, one, in effect, could produce at RT, mobility values comparable to the high mobility that exists at very low temperatures in crystals of the acene series, or at worse considerably higher than their RT mobilities. A second way involves a more drastic change in the conduction path and mechanism. It involves carrier transport via an array of single molecules, such as nanotubes or polymer chains that would bridge the gap between the source and drain electrodes of a TFT. Intermolecular transport is replaced by intramolecular transport. This would require a drastic reduction in the size of the TFT channel from micrometer-size to nanometer-size so that it is shorter than the length of a single molecule. Recently, TFTs based on carbon nanotubes have been constructed and mobilities are of the order of 100 $cm^2 V^{-1} s^{-1}$.[24] This is an excellent example of the potential effectiveness of this strategy. The successful execution of any one of these strategies would prove that the existing performance limits are partially imposed by the design and size of OTFTs, and not by the inherent properties of organic materials.

4. Modeling of the Electrical Characteristics of Organic Thin-Film Field-Effect Transistors

Figure 2 shows two common device configurations used in OTFTs. The *I–V* characteristics of OTFTs can be adequately described by models developed for inorganic semiconductors[49] as shown earlier.[7a,16,18,50–52] Polycrystalline pentacene OTFTs are used here to demonstrate typical *I–V* characteristics of OTFTs and the methods used to calculate the field effect mobility and other device parameters such as the current modulation (the ratio of the current in the accumulation mode over the current in the depletion mode, also referred to as I_{on}/I_{off} ratio), and the threshold voltage, V_T. Polycrystalline pentacene OTFTs exhibit p-type behavior (the majority carriers are holes). Thus, when the gate electrode is biased positively with respect to the grounded source electrode, they operate in the depletion mode, and the channel region is depleted of carriers resulting in high channel resistance (off state). When the gate electrode is biased negatively, they operate in the accumulation mode and a large concentration of carriers is accumulated in the transistor channel, resulting in low channel resistance (on state). For n-type TFT operation, the electrode polarity is reversed and the majority carriers are electrons instead of holes.

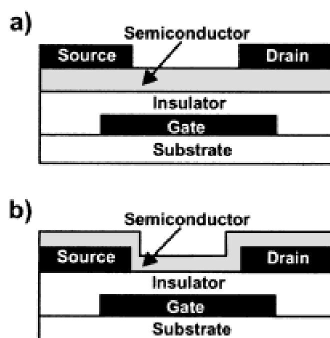

Fig. 2. OTFT device configurations: a) Top-contact device, with source and drain electrodes evaporated onto the organic semiconducting layer through a mask. b) Bottom-contact device, with the organic semiconductor deposited onto the gate insulator and the prefabricated source and drain electrodes.

A typical plot of drain current I_D versus drain voltage V_D at various gate voltages V_G is shown in Figure 3, which corresponds to a top-contact OTFT (Fig. 2a) using a polycrystalline, vapor deposited pentacene film as the semiconductor, 5000 Å thermally grown SiO_2 modified with a 1-diethoxy-1-silacyclopent-3-ene self-assembled monolayer (SAM)[53] as the gate insulator, a heavily doped n-type Si wafer as the gate, and gold source and drain electrodes.[54] At low V_D, I_D increases linearly with V_D (linear regime) and is approximately determined from the following equation:

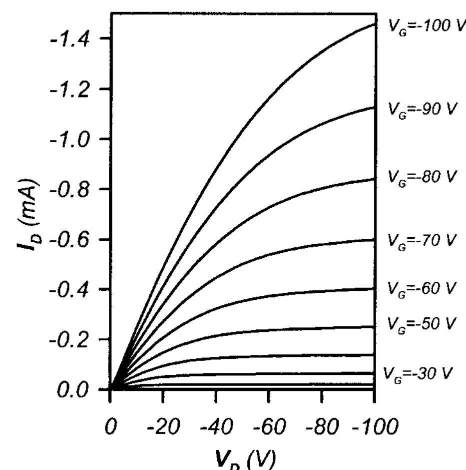

Fig. 3. Plot of a drain current I_D versus drain voltage V_D at various gate voltages V_G from a top-contact OTFT comprising a polycrystalline pentacene thin film channel, a 5000 Å thick SiO_2 gate insulator layer modified with a 1-diethoxy-1-silacyclopent-3-ene SAM, a heavily doped n-type Si wafer as the gate, and Au source and drain electrodes. The linear regime mobility is 0.80 $cm^2 V^{-1} s^{-1}$ at V_D = –10 V, and the saturation regime mobility is 1.03 $cm^2 V^{-1} s^{-1}$ at V_D = –100 V. L = 15.4 μm and W = 1 mm.

$$I_D = \frac{WC_i\mu}{L}\left(V_G - V_T - \frac{V_D}{2}\right)V_D \quad (1)$$

where L is the channel length, W is the channel width, C_i is the capacitance per unit area of the insulating layer, V_T is the threshold voltage, and μ is the field effect mobility, which can be calculated in the linear regime from the transconductance,

$$g_m = \left.\frac{\partial I_D}{\partial V_G}\right|_{V_D = \text{const.}} = \frac{WC_i}{L}\mu V_D \quad (2)$$

 © WILEY-VCH Verlag GmbH, D-69469 Weinheim, 2002 0935-9648/02/0201-0103 $ 17.50+.50/0

by plotting I_D versus V_G at a constant low V_D, with $-V_D \ll -(V_G - V_T)$, and equating the value of the slope of this plot to g_m. The calculated linear mobility value is 0.80 $cm^2\,V^{-1}\,s^{-1}$ at V_D = –10 V, which is a high value compared to previously published values of linear regime mobility from polycrystalline OTFTs. The value of V_D is chosen so that it lies in the linear part of the I_D versus V_D curve. For this device L = 15.4 μm and W = 1 mm.

For $-V_D > -(V_G - V_T)$, I_D tends to saturate (saturation regime) due to the pinch-off of the accumulation layer, and is modeled by the equation

$$I_D = \frac{WC_i\mu}{2L}(V_G - V_T)^2 \quad (3)$$

In the saturation regime, μ can be calculated from the slope of the plot of $\sqrt{|I_D|}$ versus V_G. For the same device as in Figure 3, the mobility calculated in the saturation regime was 1.03 $cm^2\,V^{-1}\,s^{-1}$, which is slightly larger than the linear regime mobility. This result is comparable to reported hole mobilities from OTFTs with polycrystalline pentacene film channels grown on SiO_2 using a substrate temperature (T_{sub}) of 120 °C during deposition[55] or on octadecyltrichlorosilane modified SiO_2 using T_{sub} of 90 °C.[38] The I_{on}/I_{off} ratio was above 2×10^6 when V_G was scanned from –100 to 0 V, and V_T was –22 V.

Figure 4 shows a graph that contains a semilogarithmic plot of I_D versus V_G and a plot of $\sqrt{|I_D|}$ versus V_G. It corresponds to a top-contact OTFT with L = 15.4 μm and width W = 500 μm, comprising pentacene as the semiconductor layer, 5000 Å thick thermally grown SiO_2 as the gate insulator, heavily doped Si (n-type) as the gate electrode and gold source, and drain electrodes. The field-effect mobility μ, calculated in the saturation regime, is 1.23 $cm^2\,V^{-1}\,s^{-1}$ at V_D = –200 V, while the threshold voltage V_T was approximately –50 V. The I_{on}/I_{off} ratio was above 1.8×10^7 when V_G was scanned from –200 to +50 V.[56] It is important to note that W/L must be at least 10 in order to minimize the effects of fringe currents flowing outside the channel, otherwise the mobility is overestimated. Alternatively, accurate mobility measurements could be obtained by patterning the semiconductor such that its width does not exceed the width of the OTFT channel.

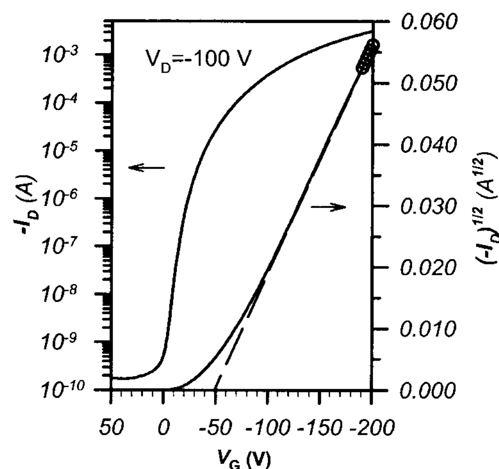

Fig. 4. Semilogarithmic plot of I_D versus V_G (left y-axis) and plot of $\sqrt{|I_D|}$ versus V_G (right axis) from a top-contact OTFT comprising a polycrystalline pentacene thin film channel, a 5000 Å thick SiO_2 gate insulator layer, a heavily doped n-type Si wafer as the gate, and Au source and drain electrodes. The field-effect mobility μ, calculated in the saturation regime, is 1.23 $cm^2\,V^{-1}\,s^{-1}$ at V_D = –200 V. L = 15.4 μm and W = 500 μm.

Strictly speaking, Equations 1 and 3 are valid only when the mobility is constant. As described below, the mobility in some OTFTs is gate bias dependent. Thus, despite of their widespread use, the above equations should only be used for estimating an approximate value of the field effect mobility in such OTFTs, and mobility values calculated this way should be treated as such. Recently, Horowitz and coworkers have developed and described a procedure for the calculation of gate field dependent mobilities in OTFTs over wide gate voltage ranges, meanwhile accounting for the series contact resistance that may exist in these devices.[57,58]

The mobility values of pentacene OTFTs most often reported in the literature are calculated in the saturation regime.[37,38,55,59] Typically, the mobility calculated in the saturation regime in pentacene OTFTs is much higher than the mobility calculated in the linear regime.[60] The linear regime mobility is more negatively affected by departures from linearity in the I_D versus V_D curves, at low V_D. Gold and other metals with even higher work functions (e.g., Pd, Pt) that are most commonly used for source and drain contacts in p-type OTFTs, form ohmic contacts with pentacene, as expected by comparing gold's work function to the valence band (or highest occupied molecular orbital, HOMO) energy level of pentacene crystals. A proof of this has been provided by comparisons of two- and four-point resistance data from pentacene OTFTs with Au contacts.[43] In addition, hole mobilities from the linear and saturation regimes calculated from single crystal field-effect transistors (FETs) of pentacene, are identical.[31] The origin of large differences between the two mobilities could be the existence of large concentrations of trap states in the channel (e.g., related to grain boundaries).

5. Vacuum Deposited Organic Semiconductor Films

Organic semiconductor films can be deposited by sublimation in a variety of vacuum deposition systems, utilizing techniques in which the deposition parameters vary widely. OTFTs with good charge carrier transport properties have been fabricated using most of these techniques. The base pressure of the deposition system is an important deposition parameter, since it determines, among other things, the mean free path of the sublimed organic semiconductor molecules, and the presence of unwanted atoms and molecules in the vicinity of the substrate surface during film formation. It ranges from less than 10^{-9} torr, in ultra high vacuum organic molecular beam deposition (OMBD),[7a] to about 10^{-7} torr for common high vacuum bell-jar deposition systems, to more

 © WILEY-VCH Verlag GmbH, D-69469 Weinheim, 2002 0935-9648/02/0201-0104 $ 17.50+.50/0

than 10^{-3} torr for simple, glass-wall vacuum sublimation systems.[61] In addition, organic sublimation systems that employ a carrier gas to transport the organic molecules from the source to the substrate have also been used.[31–33]

Substrate temperature and deposition rate are two other deposition parameters that can influence dramatically thin film morphology and thus the transport characteristics of OTFTs.[50,62]

Purity of the organic source material is also important and together with substrate cleanliness they can determine in large part the quality of an OTFT. The latter is very important since the carrier accumulation layer is occurring in the first few monolayers of the organic semiconductor at the interface with the insulator.[11,12] Impurities can affect the mobility, the on/off ratio and in some cases even the polarity of the OTFT. For example, iodine-doped pentacene is a p-type semiconductor[63] while alkaline metal-doped pentacene is an n-type semiconductor.[64]

The synthesis and fabrication of OTFTs based on polycrystalline, vapor deposited 6T[65,66] and α-ω-dihexyl-sexithiophene[67] films by Garnier et al. played a very important role in the evolution of the field of organic transistors. That work showed not only that relatively high mobilities are attainable by polycrystalline organic semiconductors, but also delineated the strategies that should be followed in order to increase the performance of OTFTs. In the case of chain- or rod-like molecules, such as thiophene oligomers, large π-conjugation length along the long axis of the molecule and close molecular packing of the molecules along at least one of the short molecular axes (π-stacking) are two important conditions for high carrier mobility. These principles are also in operation in OTFTs based on polycrystalline, vapor deposited pentacene thin films.[31,38,50,59,66]

Figure 5[50,68] contains proof of the above claims. By growing amorphous films of pentacene, which is achieved by keeping the substrate temperature close to –196 °C during deposition, a film that is practically insulating is produced. This is due to the fact that the overlap of the molecular orbitals of nn molecules is very limited because of the disorder in the solid (Fig. 5a). When the substrate temperature is kept at RT during deposition, a very highly ordered film is deposited, and the mobility measured at RT is 0.6 $cm^2 V^{-1} s^{-1}$ (Fig. 5b). The structure of this thin film is different than the structure of single crystals of pentacene, thus we must distinguish between the "thin-film phase"[50,62] and the "single-crystal phase"[69] of pentacene. When a mixture of the thin film phase and the single crystal phase is grown,[50] the mobility is very low, possibly due to the high defect concentration resulting from the coexistence of the two phases (Fig. 5c).

Figure 6 shows the morphology at the edge of a pentacene film grown on SiO_2 at RT through a shadow mask.[53] We observe that the first layer of pentacene forms single crystal islands with a lateral size of a few micrometers. Subsequent layers growing on top of these islands are smaller in size leading to a terrace-and-step morphology. The angles formed by the sides of some of the uppermost pentacene islands seem to be consistent—at the extent of accuracy that the photograph permits—with the angles of the *ab*-plane of the triclinic unit cell of pentacene.[69] Recently, photoelectron emission microscopy (PEEM) was employed to study pentacene thin film

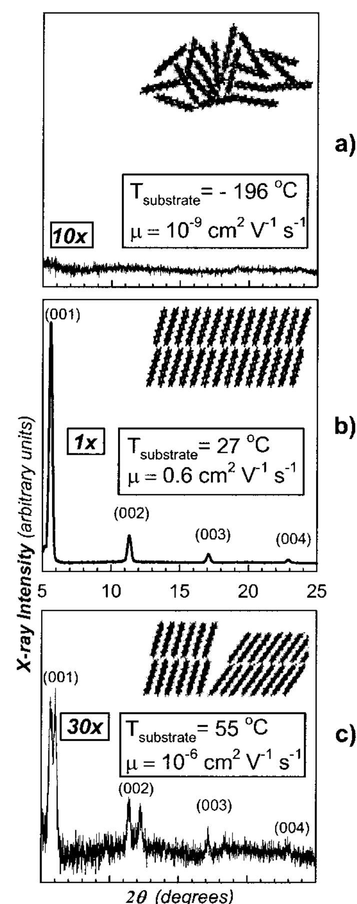

Fig. 5. X-ray diffractograms, schematic representations of structural order, and field-effect mobilities corresponding to three different thin film pentacenes. a) An amorphous phase is achieved using a substrate temperature, T_{sub} = –196 °C and a deposition rate, DR, of 0.5 Å s^{-1}. b) A single "thin film phase" [50] resulted for T_{sub} = 27 °C and DR = 1 Å s^{-1}. c) Setting T_{sub} = 55 °C and DR = 0.25 Å s^{-1} yielded a film consisting of two phases, the "thin film phase" and the "single crystal phase" [68]. Data is partially taken from [50].

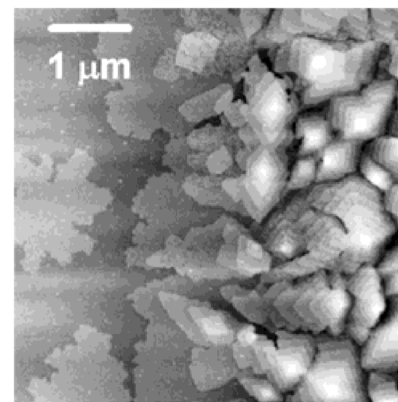

Fig. 6. Morphology at the edge of a pentacene thin film grown at RT on SiO_2 through a shadow mask. Reprinted from [53].

 © WILEY-VCH Verlag GmbH, D-69469 Weinheim, 2002 0935-9648/02/0201-0105 $ 17.50+.50/0

growth in real time and the resulting understanding contributed significantly to the identification of the pentacene growth mechanism on various surfaces.[70] Polycrystalline films of pentacene with grain sizes approaching 100 μm were fabricated on clean Si(001) surfaces passivated with a cyclohexene layer.[70] Such large grain growth can be attributed to the relatively low nucleation density of pentacene grains on such surfaces under the conditions used, which is of the order of 10^{-3} μm^{-2}, and the absence of heterogeneous nucleation on the carefully cleaned Si substrates.[70] However, the nucleation density of pentacene grains on—the technologically more important for OTFT applications—SiO_2 surface was reported to be 100 times higher than on Si(001) and cyclohexene-modified Si(001) surfaces, under the same deposition parameters.[70] Higher nucleation density generally translates to smaller grain sizes. Notably, Schön et al. have succeeded in depositing polycrystalline pentacene films on polyimide substrates with grain sizes of 100 μm using a substrate temperature below 200 °C.[31]

6. Dependence of Mobility on Gate Voltage

Pentacene TFTs have produced the highest performance among TFTs with an organic semiconducting channel (see Table 1). However, the operating voltage required to produce such performance (100 V) is usually too high, especially for portable, battery-powered device applications. We studied the gate voltage dependence of mobility in pentacene devices, and used our understanding to demonstrate high performance pentacene TFTs exhibiting mobility up to 0.4 $cm^2 V^{-1} s^{-1}$ at low operating voltages (~5 V).[39,71] An example of the dependence of mobility on V_G is shown in Figure 7, which shows plots of mobility and $\sqrt{|I_D|}$ vs. V_G for the device in Figure 4. The mobility is continuously calculated in the saturation regime for various maximum values of V_G. Clearly, there is a very strong dependence of mobility on V_G. The mobility increases from very low values (about 0.02 $cm^2 V^{-1} s^{-1}$ at V_G = –14 V) to 1.26 $cm^2 V^{-1} s^{-1}$ at –146 V. At even higher V_G the mobility reaches a plateau. The ability to set V_G as high as 200 V enabled us to reach this mobility plateau even with an OTFT comprising a relatively thick (5000 Å) SiO_2 gate insulator. This had not been possible before. Furthermore, improvements in some of the deposition parameters of the organic semiconductor, which were discussed above have resulted in much higher mobilities in the devices of Figures 3 and 4, relative to earlier pentacene devices with the same gate insulator (see for example the dotted black circles in Figure 8 which correspond to mobilities of 0.012 and 0.124 $cm^2 V^{-1} s^{-1}$ at V_G = 20 and 100 V, respectively). For comparison we note that the mobility measured at maximum gate voltage V_G = 20 and 98 V is 0.069 and 1.020 $cm^2 V^{-1} s^{-1}$, respectively (from Fig. 7).

In order to lower the operating voltage of pentacene OTFTs we have employed gate insulators with a relatively high dielectric constant (ε), such as metal oxide films of barium zirconate

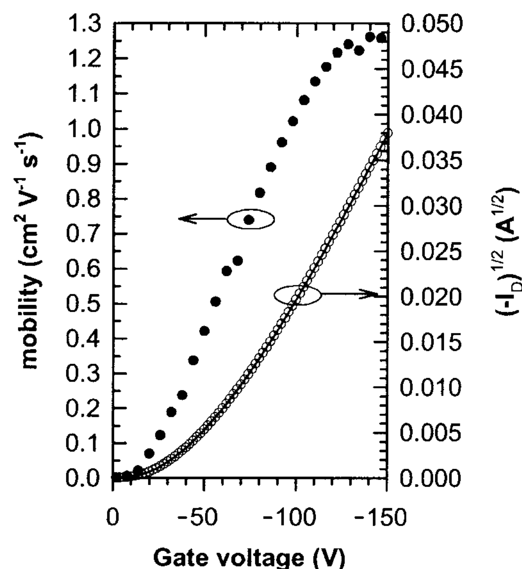

Fig. 7. Dependence of field-effect mobility of holes on V_G. Plots of mobility (left axis) and $\sqrt{|I_D|}$ (right axis) vs. V_G for the device corresponding to Figure 4.

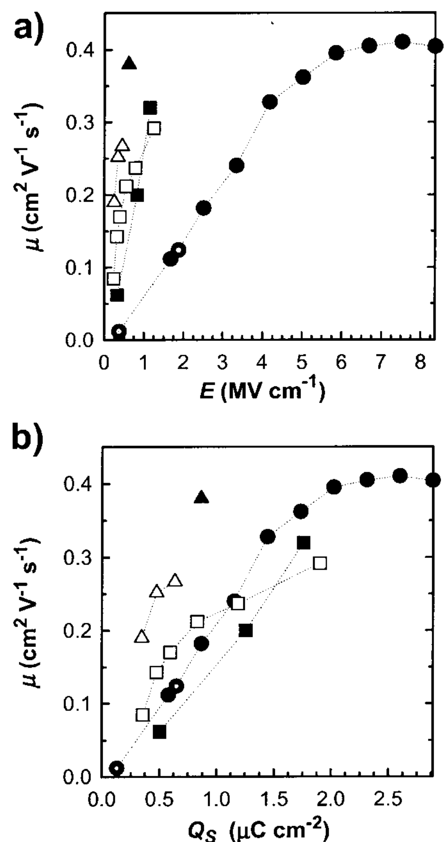

Fig. 8. a) Dependence of field-effect mobility of holes, μ, on gate field, E. b) Dependence of μ on charge per unit area, Q_S. Black or white symbols correspond to μ calculated from a gate or drain sweep, respectively. See legend for details on gate insulators. 0.5 μm SiO_2, gate sweeps (○); 0.12 μm SiO_2, gate sweeps (●); 0.082 μm BST, gate sweeps (▲); 0.090 μm BST, drain sweeps (△); 0.122 μm BZT, gate sweeps (■); 0.128 μm BZT, drain sweeps (□). The sole purpose of the dotted lines is to guide the reader's eye. Reprinted from [71].

© WILEY-VCH Verlag GmbH, D-69469 Weinheim, 2002
0935-9648/02/0201-0106 $ 17.50+.50/0

titanate (BZT),[39] or barium strontium titanate (BST)[71] Additionally, we have demonstrated the full compatibility of low operating voltage OTFTs with transparent plastic substrates by making devices on polycarbonate substrates using an all-room-temperature process sequence.[39] It is important to note here that the operating voltage can be reduced by reducing the thickness of the dielectric layer instead of increasing its dielectric constant. However, the fact that the envisioned applications for OTFTs involve almost exclusively large-area electronics, a minimum dielectric layer thickness of 1000 Å or more is dictated by reliability and manufacturing yield considerations. Thicker dielectric layers are more suitable for large area electronics applications since they suppress the formation of pinholes and the problems associated with step coverage. Thus, a higher dielectric constant gate insulator is considered the appropriate solution for high mobility pentacene OTFT with low operating voltage. Later, Gundlach et al. demonstrated pentacene OTFT devices on plastic with mobility up to 1.1 $cm^2 V^{-1} s^{-1}$ at operating voltage of about 25 V.[72]

Figures 8a and b show the dependence of field effect mobility, μ, on the gate field, E, and the charge per unit area on the semiconductor side of the insulator, Q_S, respectively.[71] Both E and Q_S are proportional to V_G. The solid black circles correspond to a pentacene-based device with a 1200 Å thick SiO_2 gate insulator thermally grown on the surface of a heavily doped n-type Si wafer that acted as the gate electrode. The dotted black circles correspond to a similar device with a 5000 Å thick SiO_2 gate insulator. The mobility for the SiO_2-based devices is calculated in the saturation regime using a gate sweep, as explained in Figure 4, and is then plotted versus the maximum V_G used in each gate sweep. The maximum V_G is varied from –20 to –100 V. During all sweeps V_D is kept constant at –100 V in order to eliminate any effects that source and drain contact imperfections might have on our results. The mobility increases linearly with increasing Q_S and E, and eventually saturates (Figs. 8b and a, respectively). Q_S is a function of the concentration of accumulated carriers in the channel region (N). Since the accumulation region has been shown in the past to be two-dimensional and confined very close to the interface of the insulator with the organic semiconductor,[11,12] all of this charge is expected to be localized within the first few semiconductor monolayers from this interface. By replacing SiO_2 with an insulator having a similar thickness but a much higher dielectric constant, an accumulated carrier concentration similar to the SiO_2 case could be attained at much lower V_G, and hence E, with all the other parameters being similar. The squares in Figure 8 correspond to devices comprising RT sputtered BZT as the gate insulator. The filled squares are generated by gate sweeps, while the open squares are generated by drain sweeps. From Figure 8a it is obvious that the applied gate field used in BST- and BZT-based devices to obtain mobility values similar to those of the SiO_2-based devices was about five times lower compared to the fields used in the latter devices. This clearly proves that high field is not required to obtain high mobility. Thus, the gate voltage dependence of mobility in these devices is due to the higher concentration of holes accumulated in the channel. Figure 8b, which plots μ versus charge per unit area, Q_S, corroborates this conclusion. The values of Q_S and N required to reach a certain mobility value are practically the same for SiO_2- and BZT-based devices although much different gate voltage and gate field values were required to obtain such a mobility in each case.

The gate voltage dependence of mobility in vacuum deposited pentacene OTFTs was first reported in one of our previous publications.[50] A similar behavior was later reported for pentacene OTFTs deposited from solution via the precursor route (see below).[73] The multiple trapping and release (MTR) model,[74] which is widely used to model the behavior of a-Si:H TFT seems to be a likely mechanism that explains the observed characteristics in vapor deposited polycrystalline films of pentacene. This model, which is based on the assumption that the intrinsic charge transport mechanism is one involving extended states, has been successfully used in the past to model the field dependence of mobility in 6T and α,ω-dihexyl-sexithiophene (DH6T) OTFTs.[18,39,58,71,75,76] According to this model a distribution of traps exists in the forbidden gap above the valence band edge. At low gate bias most of the holes injected in the semiconductor are trapped into these localized states. The deepest traps are filled first and carriers can be released thermally. As the negative gate bias increases, the Fermi level approaches the valence band edge as more traps are filled. At an appropriately high voltage all trap states are filled and any subsequently injected carriers move with the microscopic mobility associated with carriers in the valence band.[39,71] Several trap levels have been reported for thin polycrystalline vapor deposited films of pentacene at depths ranging from 0.06 eV to 0.68 eV,[77] which could account for the traps described in the MTR model. Traps can be linked to impurities, and various structural defects in the crystalline structure of the pentacene film, including point defects, dislocations, and most importantly grain boundaries. Schön et al. have used the concept of positively charged grain boundaries to explain the gate voltage dependence of mobility in polycrystalline pentacene films.[31] An energy barrier is created at the grain boundaries and is a function of the charged trapping states at the boundaries, the carrier concentration within the grains and the temperature.[31] The effective mobility across two grains of tetracene that are separated by a grain boundary is given by: $\mu^{-1} = \mu_G{}^{-1} + \mu_{GB}{}^{-1}$, where μ_G is the single crystal mobility (intragrain mobility) and μ_{GB} is the mobility across the grain boundary.[78] The charge transport is dominated by thermionic emission over the potential barrier at the grain boundary from 20 to 150 K, and by the intragrain transport (μ_G) above 150 K. From 4 to about 20 K transport is dominated by tunneling of charge carriers through the potential barrier at the grain boundary. Chwang and Frisbie have shown that carrier transport in 6T OTFTs is limited by the presence of grain boundaries in the channel.[79] Their experiments involved transport measurements through single grain boundaries in vapor deposited 6T and showed that transport is dependent on carrier concentration exhibiting decreasing

 © WILEY-VCH Verlag GmbH, D-69469 Weinheim, 2002 0935-9648/02/0201-0107 $ 17.50+.50/0

activation energy with increasing carrier concentration. Another important conclusion of that work is that larger threshold voltages in OTFTs correlate with larger trap densities at grain boundaries.[79]

Vissenberg and Matters have studied theoretically the field effect mobility in OTFTs comprising amorphous organic semiconductor channels, and have successfully used percolation theory and the concept of transport by carrier hopping in an exponential density of localized states to model the experimentally obtained gate voltage and temperature dependence of mobility from such OTFTs.[80] It should be mentioned here that hopping transport models differ substantially from models like MTR that assume delocalized transport limited by traps or grain boundaries. They showed that the mobility dependence on temperature in such OTFTs exhibits a simple Arrhenius behavior, with a gate voltage dependent activation energy. According to this model, the differences in the magnitude and temperature dependence of the mobility in pentacene and polythienylenevinylene (PTV) transistors are mainly due to differences in the structural order of the organic semiconductor channels.[80]

Yu et al. have proposed a model that successfully explains field and carrier density dependences of the mobility in films of conjugated organics, both in low-field/high carrier concentration cases (OTFTs), and in high-field/low carrier concentration cases (organic diodes). This model is based on the assumptions that thermal fluctuations modify the energy levels of polaronic electronic states, and that the primary restoring force for these fluctuations is steric, which leads to spatial correlation in the energies of the localized electronic states.[81]

Pentacene transistor drain–source contacts can be made in one of two configurations (Figs. 2a and b): top contact and bottom contact. The performance of pentacene devices with the bottom contact configuration is inferior to that of devices with the top contact configuration. Consequently, most high-performance pentacene TFTs reported in the literature have the top contact configuration, and shadow masking is generally used to pattern the source and drain contacts on top of the pentacene. Unfortunately, this is a process that cannot be used in manufacturing, hence a protocol that allows the photolithographic patterning of the source and drain electrodes on the insulator before the deposition of pentacene, according to the schematic shown in Figure 2b, had to be developed. Furthermore, the performance of devices fabricated with such a process should be similar if not better than that of top contact devices (Fig. 2a).

Figure 9 shows a pentacene layer as it was grown on SiO_2 and a Au electrode.[82] The edge between SiO_2 and Au is marked by the end of the white in the middle photograph area that corresponds to Au (due to variations in image contrast, the pentacene-covered Au appears different in the top two pictures). On SiO_2, far away from the Au edge, pentacene consists of fairly large grains (having sizes between 0.2 and 0.5 μm). On Au the grain size is dramatically reduced. This small crystal growth persists into the channel region (on SiO_2).[82–84] Close to the Au edge but on the SiO_2 side there is a transition region where the grain size increases with increasing distance from

Fig. 9. Scanning electron microscopy (SEM) image of a pentacene thin film grown on SiO_2 and a Au electrode. The grain size is much smaller on Au than on SiO_2 far from the Au edge. The pentacene grain size on SiO_2 in the region close to the Au edge is similar to that on Au and increases with increasing distance from the edge. Reprinted from [82].

the edge. It is the morphology of the pentacene film in the OTFT channel region close to the electrode edge that causes the performance limitation of the bottom contact TFT. Right at the edge of the Au electrode, there is an area with very small crystals and hence a large number of grain boundaries. Grain boundaries are high-volume and low-order regions that contain many morphological defects, which in turn are linked to the creation of charge carrier traps with levels lying in the band-gap. These defects can be considered responsible for the reduced performance of bottom contact pentacene TFTs. The reduction of their concentration to levels similar to those in the area at the center of the channel (lower part of Fig. 9) should result in bottom contact devices with performance similar to or better than that of top contact devices. In a typical bottom contact pentacene TFT the mobility is equal to or less than 0.16 $cm^2 V^{-1} s^{-1}$. We have used a SAM of 1-hexadecane thiol to modify the surface energy of the Au electrode in an effort to improve the crystal size and ordering of the pentacene overgrowth.[84] Mobilities calculated in saturation from such

 © WILEY-VCH Verlag GmbH, D-69469 Weinheim, 2002 0935-9648/02/0201-0108 $ 17.50+.50/0

devices were up to 0.48 $cm^2 V^{-1} s^{-1}$, which is three times larger than the mobility of devices with untreated Au electrodes. Mobilities calculated in the linear regime were up to 5 times higher in devices treated with a SAM vs. untreated devices.[84] The pentacene layers for both devices were deposited in the same deposition run. Figure 10 provides an explanation for the improvement in device performance.[84] The SAM deposited on Au resulted in a pentacene grain size on Au similar to the large grains grown on the SiO_2 in the center of the channel.

Fig. 10. SEM image of a pentacene thin film grown on SiO_2 and a Au electrode covered with a SAM of 1-hexadecane thiol. A similar grain size on both the SiO_2 and the Au/SAM surface is observed. The pentacene grain size transition region at the Au edge is eliminated. Reprinted from [84].

There is no transition region at the Au edge, hence the trap concentration must have been drastically reduced. As described in more detail in the section on n-type OTFTs below, the SAM may have the additional effect of altering the apparent workfunction of the metal electrode relative to the organic semiconductor HOMO and lowest unoccupied molecular orbital (LUMO). This could affect the carrier injection characteristics from the contacts to the organic semiconductor and thus alter the overall performance of OTFTs. However, in the specific case of pentacene OTFTs it has been shown previously that Au forms ohmic contacts to pentacene (see above).[43] Thus the presence of a SAM could only make hole injection less efficient if it shifted the apparent workfunction of Au to lower values compared to an unmodified Au surface. If, on the other hand, it shifted it to higher values, it would not significantly effect hole injection, since the contact of unmodified Au to pentacene is ohmic. Thus, we do not believe that changes in gold's apparent workfunction due to deposition of a SAM play an important role in the improvement of the performance of pentacene OTFTs comprising SAM modified Au source and drain electrodes.

7. Solution Processed Organic Semiconductor Films

The technology that is believed to have the potential to produce the highest impact on manufacturing costs is the use of soluble organic semiconductors, both polymers and oligomers, combined with large area stamping or printing techniques that could eliminate lithography. Below, we summarize some important recent developments in this field.

One of the first solution-processable organic semiconductors used for FETs was poly(3-hexylthiophene) or P3HT, in which the addition of alkyl side-chains enhanced the solubility of the polymer chains.[85] P3HT films spun from a chloroform solution had mobilities in the range of 10^{-5} to 10^{-4} $cm^2 V^{-1} s^{-1}$. These mobilities were comparable to the mobilities obtained from electrochemically-prepared polythiophene FETs,[86] indicating that the incorporation of insulating alkyl side chains was not detrimental to the electronic properties of polythiophene. A comparison study of poly(3-alkylthiophene)s with side chains ranging in length from butyl to decyl showed that field-effect mobility decreases with increasing chain length.[87] For films spun from chloroform, mobilities ranged from 1–2 × 10^{-4} $cm^2 V^{-1} s^{-1}$ for poly(3-butylthiophene) and P3HT down to 6×10^{-7} $cm^2 V^{-1} s^{-1}$ for poly(3-decylthiophene).

When regioregular P3HT[88] consisting of 98.5 % or more head-to-tail (HT) linkages (Scheme 1) was used to fabricate FETs, a dramatic increase in mobility was observed relative to regiorandom poly(3-alkylthiophene)s.[89] Mobilities as high as 0.045 $cm^2 V^{-1} s^{-1}$ were achieved in films drop-cast from a chloroform solution.[89] Drop cast films of highly regioregular P3HT self-orient into a well-ordered lamellar structure with an edge-on orientation of the thiophene rings relative to the substrate.[88] This is in contrast to solution cast films of regiorandom poly(3-alkylthiophene)s, which are essentially amorphous.[88] Spin-coated films of regioregular P3HT are

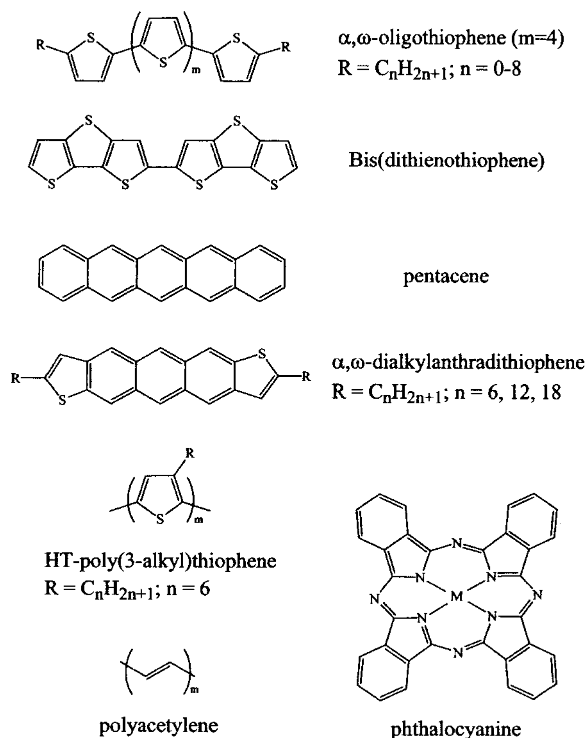

Scheme 1. Molecular structures of common p-type organic semiconductors.

 © WILEY-VCH Verlag GmbH, D-69469 Weinheim, 2002 0935-9648/02/0201-0109 $ 17.50+.50/0

also well ordered, but the lamellae adopt different orientations depending on the degree of regioregularity.[90] Highly regioregular P3HT (greater than 91 % HT linkages) also forms lamellae with an edge-on orientation (π–π stacking direction in the plane of the substrate) when spun from chloroform. Mobilities of 0.05 to 0.1 $cm^2 V^{-1} s^{-1}$ were obtained for 96 % regioregular P3HT.[90] In contrast, spin-coated films of P3HT with low regioregularity (81 % HT linkages) consisted of lamellae having a face-on orientation (π–π stacking direction perpendicular to the substrate) and resulted in mobility of 2×10^{-4} $cm^2 V^{-1} s^{-1}$. Drop cast films of 81 % regioregular P3HT adopted an edge-on lamellar structure, resulting in an order-of-magnitude increase in mobility compared to spin-coated films. This study indicates that, in addition to the degree of order in the polymer film, the π–π* stacking direction relative to the substrate, which depends on the film deposition method, greatly affects the field-effect mobility.[90] This is reasonable, since the edge on lamellar structure ensures that delocalized intermolecular states are formed in the direction parallel to the substrate, which happened to be the transport direction in OTFT devices.

The mobility of regioregular P3HT has been found to vary by two orders of magnitude depending on the solvent used, with chloroform giving the highest mobility.[89] Modification of the substrate surface prior to deposition of regioregular poly(3-alkylthiophene) has also been found to influence film morphology. For example, treatment of SiO_2 with hexamethyldisilazane (HMDS) or an alkyltrichlorosilane replaces the hydroxyl groups at the SiO_2 surface with methyl or alkyl groups. The apolar nature of these groups apparently attracts the hexyl side chains of P3HT, favoring lamellae with an edge-on orientation. Mobilities of 0.05 to 0.1 $cm^2 V^{-1} s^{-1}$ from highly regioregular P3HT have been attributed to this surface modification process.[91,92] In addition, it has been shown that top contact devices yield mobilities that are typically larger by a factor of two compared to bottom contact devices.[91,93] Exposure of poly(3-alkylthiophene) films to air causes an increase in conductivity and a subsequent degradation of the transistor on/off ratio. This is the result of doping with oxygen (doping by water is a less probable but possible cause), since it is possible to achieve high on/off ratios by preparing and testing devices in a dry N_2 atmosphere.[91,93] Gate induced superconductivity in a polymer was recently reported in drop cast, bottom contact P3HT TFT, at $T \leq 2.35$ K, and at sheet carrier densities exceeding 2.5×10^{14} cm^{-2}, demonstrating for the first time that the properties of organic polymers can be tuned from insulating to semiconducting, to metallic and finally to superconducting.[94] Superconductivity had been observed in the past in crystalline inorganic polymers,[95] and one-dimensional stacks of non-polymeric, conducting organic salts such as tetramethyltetraselenafulvalene (TMTSF), which were the first organic conductors to exhibit superconductivity.[96]

Sirringhaus et al. have recently demonstrated direct inkjet printing of OTFTs based on solution-processed polymer electrodes (water-soluble poly[3,4-ethylenedioxythiophene] doped with polystyrene sulfonic acid (PEDOT/PSS)), insulators (polyimide), and active organic semiconducting layer (poly[9,9-dioctylfluorene-*co*-bithiophene], called F8T2, from xylene solution).[97] It was shown that F8T2, which is a nematic liquid crystalline conjugated polymer semiconductor, can be preferentially oriented by rubbed polyimide layers, and when used as the active channel in OTFTs it exhibits a mobility of 0.02 $cm^2 V^{-1} s^{-1}$ and an on/off ratio of 10^5.[97,98]

While spin coating, solution casting and printing are perhaps the most commercially feasible processing techniques for soluble polymeric semiconductors, the Langmuir–Blodgett (LB) technique and its variations have also been explored for the preparation of poly(3-alkylthiophene) FETs.[99–102] The maximum mobility measured from multilayer LB films of P3HT was 0.02 $cm^2 V^{-1} s^{-1}$.[101]

Unsubstituted quinquethiophene and end-substituted quater-, quinque-, and sexithiophene display enough solubility in organic solvents to allow fabrication of field-effect devices by solution processing techniques. Initial studies of solution-processed oligothiophene transistors gave mobilities of ~5×10^{-5} $cm^2 V^{-1} s^{-1}$ for quinquethiophene and α,α'-diethylquaterthiophene (DE4T).[103] More recently, mobilities in the range of 0.01 to 0.1 $cm^2 V^{-1} s^{-1}$ have been achieved using solution processed substituted oligothiophenes.[104–107] The mobility was found to depend strongly on film morphology, which can be controlled by processing conditions, such as solution concentration, substrate temperature during casting, solvent choice, and environmental conditions during film drying.

Other soluble organic oligomers have also been investigated as semiconducting materials for FETs. Anthradithiophene, a fused heterocycle compound, is soluble in its dihexyl end-substituted form. Dihexylanthradithiophene (DHADT) transistors were fabricated by solution casting from hot chlorobenzene, followed by evaporation of the solvent in a vacuum oven at various temperatures. The electrical characteristics of the films were strongly dependent on the temperature during film drying. The highest mobilities, 0.01 to 0.02 $cm^2 V^{-1} s^{-1}$, were obtained for a drying temperature of 100 °C.[106,108] In comparison, vacuum evaporated films of DHADT gave mobilities as high as 0.15 $cm^2 V^{-1} s^{-1}$.[108]

Transistors utilizing another thiophene-containing oligomer, *trans–trans*-2,5-bis[2-{5-(2,2′-bithienyl)}ethenyl]thiophene (BTET), were fabricated by spin coating from hot *N*-methyl pyrrolidinone (NMP). The mobility of such a device was 1.4×10^{-3} $cm^2 V^{-1} s^{-1}$ compared to 0.012 $cm^2 V^{-1} s^{-1}$ for a vacuum evaporated device.[109]

Although a great deal of success has been achieved with soluble oligomers, the solubility of these oligomers is low, requiring the solvents to be heated. Drop casting and spinning yield films that are non-uniform in thickness, morphology, and electrical properties. To circumvent such problems, another approach to solution processable oligomeric materials has been developed that involves a soluble precursor molecule that is not semiconducting, and which can be converted to its semiconducting insoluble form upon heating. This approach has been realized for pentacene, with initial reported mobili-

 © WILEY-VCH Verlag GmbH, D-69469 Weinheim, 2002 0935-9648/02/0201-0110 $ 17.50+.50/0

ties of 0.01 to 0.03 cm^2 V^{-1} s^{-1}.[16,110,111] The pentacene precursor is soluble in dichloromethane and forms continuous, amorphous films when spun onto substrates. The conversion to pentacene is accomplished by heating the films to a temperature of 140–220 °C in vacuum. Tetrachlorobenzene is eliminated in the conversion process. In a more recent study, a mobility of 0.2 cm^2 V^{-1} s^{-1} was achieved by treatment of the SiO_2 substrate with HMDS prior to spin coating the precursor, and by optimizing the conversion conditions. Precursor films were formed by spin coating from a 1.5 wt.-% solution in dichloromethane, and heating the film for 5 s at 200 °C followed by rapid quenching.[112]

The precursor approach has also been applied to polymers. In fact, one of the first reported transistors based on organic polymer channels used precursor-route polyacetylene as the semiconducting layer.[113,114] Another polymeric semiconductor that has been processed from a soluble precursor polymer is PTV.[16,30,86,111]

8. N-Type Organic Semiconductors

High performance n-type materials will enable the fabrication of p–n junctions, as well as complementary logic circuits. It's interesting to note that most of the work to date has focused on p-type organic materials such as pentacene, poly(3-alkylthiophene), or oligothiophenes, which were described in the previous section, whereas only recently has any serious effort been guided towards the preparation of novel n-type semiconductor materials. The disproportionate development of p-type organic FETS (OFETs) vs. n-type is clearly the result of the inherent instability of organic anions, in particular carbanions, that react with oxygen and water under operating conditions, thus providing unstable devices.

De Leeuw et al. have indirectly addressed this issue by examining the stability of n-type doped (i.e., reduced) polymers and by evaluating standard redox potentials for reactions with water and oxygen.[115] He concluded that although there is an optimum thermodynamic stability window that can be determined based on standard redox potentials, the stability of n-type doped materials depends strongly on the value of the overpotential (i.e., free energy of activation) associated with the chemical processes (i.e., reaction with either water or oxygen).[116] Therefore, careful tuning of the electron affinity of n-type materials will have to be done in order to obtain thermodynamically stable devices, otherwise passivating layers or encapsulants will have to be employed. Alternatively, air stability could be achieved by kinetically inhibiting the undesired redox processes. For instance, the incorporation of hydrophobic functionalities into the chemical structure of the organic semiconductor could prevent the penetration of water, thus providing a "kinetic" barrier.

Design rules for n-type organic semiconductors are very similar to p-type materials except that n-type devices must utilize semiconductor materials that allow the injection of electrons into its LUMO. Therefore, the electron affinity of the semiconductor should be optimized such that the LUMO level (conduction band) offset with respect to the Fermi level of the source and drain electrodes does not limit the injection of electrons from the source into the semiconductor and from the semiconductor into the drain. Most of the work done to date has employed gold electrodes as the source and drain. Gold has a work function of ~5.0 eV against vacuum and since most n-type materials have solid state electron affinity levels ~4.0 eV, this energy barrier of approximately 1 eV would be expected to severely limit charge injection into the semiconductor. Interestingly, this is not the case. What is known is that when gold surfaces are coated with organic materials, the apparent workfunction of the metal can change by up to 1 eV, thus facilitating the injection of charge into n-type materials.[117] Alternatively, this apparent workfunction change can be interpreted in terms of an ultrathin, interfacial electric dipole layer that in effect results in a vacuum level shift at the metal/organic interface.[118] This phenomenon ultimately introduces another element of complexity in terms of attempting to match the workfunction of the electrodes with the intended semiconductor conduction band in order to produce ohmic contacts.

The literature on n-type OTFTs takes us back only 10 years. Table 2 lists the highest field-effect mobility (μ) values measured from n-type OTFTs as reported in the literature, annually from 1990 to the present time, for each one of the most promising n-type organic semiconductors. Figure 11 graphically conveys the information contained in Table 2. The various n-type materials are grouped together, when possible, taking into consideration only the core part of each molecule and not the specific substituents.

Table 2. The highest field-effect mobility (μ) values measured from n-type OTFTs as reported in the literature, annually from 1990 to the present time, for each one of the most promising n-type organic semiconductors.

Year	Mobility [cm^2 V^{-1} s^{-1}]	Material	I_{on}/I_{off}	W/L	Reference
1990	2×10^{-4}	Pc_2Lu	NR	0.1 cm/50 μm	[119]
1990	1.4×10^{-3}	Pc_2Tm	NR	0.1 cm/50 μm	[119]
1993	10^{-4}	C_{60}/C_{70} (9:1)	NR	8 cm/5 μm	[148]
1994	3×10^{-5}	TCNQ	4-450 [a]	10 mm/5 μm	[120]
1995	0.08	C_{60}	10^6	400	[121]
	0.3		22	400	
1996	1.5×10^{-5}	PTCDI-Ph	NR	0.5 cm/50 μm	[127]
1996	0.003	TCNNQ	8 [b]	250 μm/12 μm [b]	[124]
1996	10^{-4}	NTCDI	10^2 [b]	250 μm/12 μm [b]	[124]
1996	0.003	NTCDA	10^3 [b]	250 μm/12 μm	[124]
1997	10^{-4}-10^{-5}	PTCDA	NR [b]	250 μm/12 μm	[128]
1998	0.03	F16CuPc	5×10^4	250 μm/12 μm	[137]
2000	0.06	NTCDI-C8F	10^5	17	[125]
	0.1			1.5	
2000	0.02	DHF-6T	10^5	1.5 mm/75 μm	[139]
	0.5	Pentacene	NR	10-100	[31]
2001	0.6	PTCDI-C8	10^5	1500 μm/95 μm	[61]

[a] On/off ratio increases upon exposure to air. [b] Personal communication.

Early work in this area provided some devices with respectable mobilities and on/off ratios yet they were unstable in air. Some materials provided devices with limited air stability but charge transport properties were poor and none of these materials were soluble enough to be processed from solution.

 © WILEY-VCH Verlag GmbH, D-69469 Weinheim, 2002 0935-9648/02/0201-0111 $ 17.50+.50/0

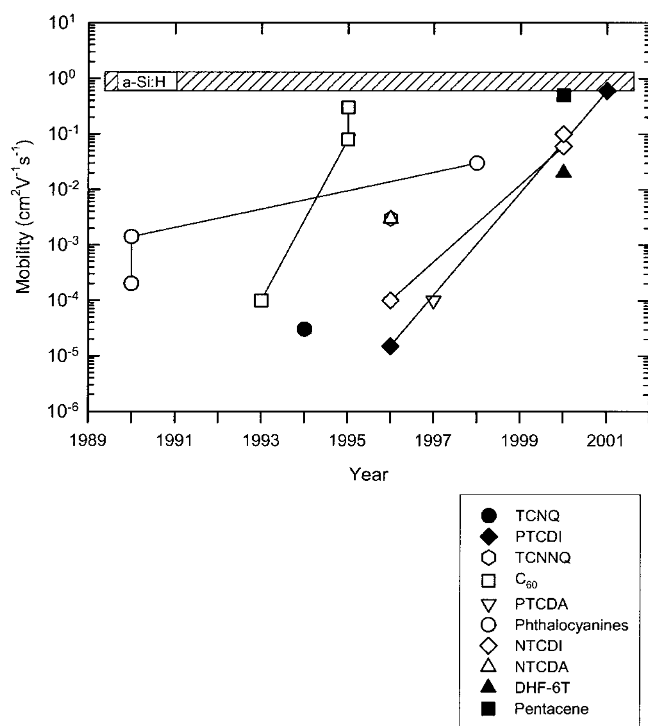

Fig. 11. Evolution of OTFT mobility for the most common n-type organic semiconductors. The various n-type materials are grouped together into families of similar molecules taking into account only the core part of each molecule. For reference, a representative range of electron mobilities for a-Si:H TFT is shown.

Recently, researchers have been able to obtain materials that provide devices with most of the requisite properties such as high mobility and current on/off ratio as well as stable operation in air, and solution processability. The remainder of this review is intended to summarize the area of n-type OTFTs by focusing on charge transport characteristics as well as the effect of deposition conditions on morphology and device performance. The organization is for the most part chronological, while individual sections are distinguished by the basic chemical structure of the semiconductor materials used for OTFT fabrication.

The earliest study on n-type OTFTs was undertaken by Guillaud and co-workers and involved lutetium (Pc_2Lu) and thulium (Pc_2Tm) bisphthalocyanines.[119] Device stability is excellent under vacuum at RT, therefore electrical measurements were made in situ, without breaking vacuum at any point in time during the process of fabrication. N-type mobilities of 10^{-3}–10^{-4} for both Pc_2Tm and Pc_2Lu were obtained in vacuo. Interestingly, upon exposure to air, only p-type activity was observed.

Brown and co-workers have explored the use of tetracyanoquinodimethane (TCNQ) as the active material in an n-type OTFT.[120] Bottom contact devices were fabricated with gold electrodes. TCNQ has a reduction potential of +0.19 V versus the standard calomel electrode. This is in the same region as the oxidation of p-type materials that are known to make ohmic contacts with gold. Hence, the LUMO level of TCNQ is expected to be in the vicinity of the Fermi level of the gold contacts, thus allowing for facile electron injection into TCNQ. Nevertheless, very poor devices provided a mobility of 3×10^{-5} $cm^2 V^{-1} s^{-1}$ and an on/off ratio up to 450 upon exposure to air (4 to 450).

Haddon et al. have explored the use of C_{60} as the semiconducting material in n-type FET devices.[121] C_{60} films were deposited under ultra high vacuum (UHV) such that no exposure to oxygen occurred. Such films consist of random polycrystalline grains of approximately 60 Å in size. Chromium and gold electrodes were used. In separate experiments it was shown that Cr electrodes lead to higher conductivities and create more carriers at the C_{60}/Cr interface than Au/Cr double layers. C_{60} devices are sensitive to amine exposure and pretreatment of the substrate with tetrakis(dimethylamino)ethylene (TDAE) prior to deposition of C_{60} moves the threshold voltage to negative values (the device does not turn off at 0 V) and increases the FET mobility by a factor of 3 (μ = 0.08 to 0.3 $cm^2 V^{-1} s^{-1}$) at the expense of the current on/off ratio. It has been shown in previous work[122] that C_{60} can be reduced by TDAE, thus doping is likely to be the cause of the increase in mobility and concomitantly the increase in off-current.

Unfortunately, C_{60} devices could not be operated in air. Their resistivity quickly increased 4–5 orders of magnitude. Their operation could be restored upon placing the devices in a UHV chamber at elevated temperature overnight. This suggests that oxygen acts as electron traps within the C_{60} lattice. TOF measurements for C_{60} single crystals[123] have shown mobilities of 0.5 $cm^2 V^{-1} s^{-1}$, thus, as expected from the discussion in a previous section, the grain boundaries lower the mobility in thin evaporated films. Isotropic films of C_{60} provide good device characteristics, in contrast to other materials that require special consideration in order to obtain highly ordered structures. This may be related to the approximately spherical shape of C_{60} as opposed to the rigid rod shape or more generally elongated shape of most of the other organic semiconductors.

Katz and co-workers have explored several materials based on the naphthalene framework (see Scheme 2).[104,124] Initially explored was 1,4,5,8-naphthalene tetracarboxylic dianhydride (NTCDA) in which mobilities of 1–3 × 10^{-3} $cm^2 V^{-1} s^{-1}$ were measured for materials deposited onto substrates held at 55 °C. Upon exposure to air the mobility decreases by 1–2 orders of magnitude. Lower mobilities are observed when devices are exposed to atmospheric moisture after sublimation. At substrate temperatures of 25 °C mobilities of 10^{-4} $cm^2 V^{-1} s^{-1}$ were observed. Although similar grain sizes (200 nm) are obtained for both temperatures, films deposited at 55 °C were more continuous. Devices constructed from 1,4,5,8-naphthalene tetracarboxylic diimide (NTCDI) provided mobilities on the order of 10^{-4} $cm^2 V^{-1} s^{-1}$. Lastly, 11,11,12,12-tetracyanonaphtho-2,6-quinodimethane (TCNNQ) devices display higher mobilities (10^{-3}) than TCNQ[120] (vide infra), while having better air-stability than NTCDA. Unfortunately, a high off current is observed, presumably due to unintentional doping, thus providing devices with poor on/off ratios.

 © WILEY-VCH Verlag GmbH, D-69469 Weinheim, 2002 0935-9648/02/0201-0112 $ 17.50+.50/0

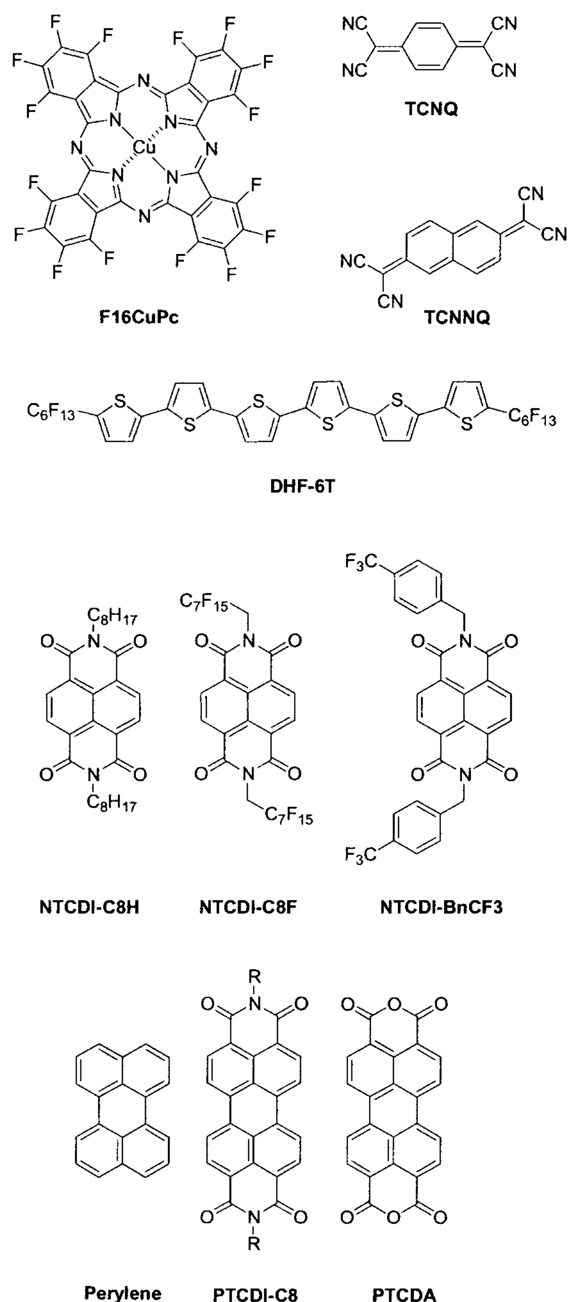

Scheme 2. Molecular structures of common n-type organic semiconductors.

Recently, Katz and co-workers reported the fabrication of n-type OTFTs comprising a series of materials based on *N,N'*-dialkyl-naphthalene-1,4,5,8-tetracarboxylic diimide (see Scheme 2).[125] In this study, the transport characteristics varied greatly with substitution. For instance, only the fluorinated materials (NTCDI-C8F, NTCDI-BnCF3) showed high mobilities in air, whereas mobilities of 0.001–0.1 were found for linear, alkyl functionalized diimides (NTCDI-C8H, NTCDI-C12H, NTCDI-C18H), but only under vacuum. The highest mobility in air (>0.1 $cm^2 V^{-1} s^{-1}$) was obtained with NTCDI-BnCF3, while the highest on/off ratio in air (>10^5) was achieved with NTCDI-C8F. As observed with many other organic semiconductors, mobilities were generally much higher when the material was deposited onto a substrate at elevated temperature. Alternative electrodes were examined and carbon electrodes gave similar results to gold electrodes yet not as reproducible. Furthermore, carbon could be used in a bottom contact configuration where as gold generally failed even if cleaned with oxygen plasma. Interestingly, aluminum electrodes did not provide active devices. Although this is likely due to oxidation of aluminum, it is important to note that organic films on low workfunction metals can also alter the effective workfunction, in this case increasing it, thus making it less favorable for injection.[117] Since bottom contact devices rarely produced transistor activity, the use of thiols to modify the gold surface was explored. Excellent results were obtained using 3,4-dichlorobenzyl mercaptan. Currents as high as 100 μA were observed for NTCDI-BnCF3, providing a mobility of ca. 0.1 $cm^2 V^{-1} s^{-1}$ for bottom contact devices (T_{dep} = 90–100 °C). It has been shown that functionalizing the surface of gold with thiols can result in a modified work function,[117] yet the presence of an organic monolayer may also facilitate the ordering of the semiconductor upon deposition, such that the grain boundaries are reduced at the channel/electrode interface as previously seen with pentacene devices (vide supra). NTCDI-C8F is soluble in hot α,α,α-trifluorotoluene, and solution casting results in morphologically non-uniform films, with some regions of the films giving mobilities greater than 0.01 $cm^2 V^{-1} s^{-1}$.

The gate voltage could be cycled in air for up to 1 h as long as the voltage remained below 50 V. Interestingly, the redox data does not show a significant difference between fluorinated and non-fluorinated derivatives, yet there is clearly a difference in their performance in air. Also, the potentials measured are formally outside the stability window described by de Leeuw,[115] thus indicating that air stability can be obtained even with materials that are expected to be unstable thermodynamically. Since thin film orientation and layer spacings are similar for fluorinated and non-fluorinated analogs, solid-state structural characteristics were examined.[126] In the case of the linear side-chains, the dense packing of the fluorinated side-chains (e.g., NTCDI-C8F) vs. aliphatic side-chains (e.g., NTCDI-C8H) could provide a “kinetic” barrier to atmospheric contaminants. Consistent with this hypothesis, is the relatively lower stability of the less densely packed NTCDI-BnCF3 derivative vs. NTCDI-C8F, yet such an argument is not so straight forward when comparing NTCDI-BnCF3 to NTCDI-BnCH3, in which the former provides air stable devices yet the later has mobilities on the order of 10^{-5} $cm^2 V^{-1} s^{-1}$ even under vacuum. It is also interesting to note the dramatic stability difference observed between single crystals of NTCDI-BnCF3 and NTCDI-BnCH3. The subtle packing differences in the single crystal may account for the significantly lower activation energy required to fill trapping levels in the NTCDI-BnCF3 derivative, thus providing better device performance. Clearly, similar film morphologies do not extrapolate to comparable device performance such as mobility and current on/off ratios.

 © WILEY-VCH Verlag GmbH, D-69469 Weinheim, 2002 0935-9648/02/0201-0113 $ 17.50+.50/0

Garnier and co-workers have explored the n-type charge carrier characteristics of *N,N′*-diphenyl-3,4,9,10 perylenetetracarboxylic diimide (PTCDI-Ph) where an electron mobility of 1.5×10^{-5} cm^2 V^{-1} s^{-1} was measured.[127] Gold and aluminum contacts were used in a bottom contact configuration, yet aluminum electrodes were found to have 3 times lower performance. Devices degraded rapidly in air and the field effect was lost after two to three days with gold devices, and even faster with aluminum. Faster degradation of the aluminum devices is most likely due to the compounded effect of oxidation at the electrodes as well as the incorporation of moisture and/or oxygen into the film.

Studies with 3,4,9,10-perylenetetracarboxylic dianhydride (PTCDA) also produced devices with poor transport characteristics where mobilities of 10^{-4}–10^{-5} cm^2 V^{-1} s^{-1} were obtained.[128] It is important to note that the orientation of PTCDA on a surface depends strongly on the deposition conditions used.[129] Films of PTCDA grown on gold were found to grow quasiepitaxially under specific conditions, thus resulting in highly ordered films.[130] Such low mobilities are ascribed to limited electronic orbital overlap in the direction of transport. Furthermore, PTCDA OTFTs do not operate in wet air, yet in vacuo or under dry oxygen they perform as described previously (vide supra) and the effect of moisture on the devices is reversible. Karl and Marktanner have shown using TOF experiments that the electron mobility in polycrystalline thin films PTCDA is inversely proportional to the width of the X-ray rocking curve from the thin film.[131,132] The maximum mobility reported was 3×10^{-2} cm^2 V^{-1} s^{-1}.[131,132]

In a recent study, Schön et al. demonstrated the feasibility of using a perylene single crystal as the active material in an OFET device.[133] Mobilities of 5.5 cm^2 V^{-1} s^{-1} were measured at RT. At low temperatures, mobilities as high as 120 cm^2 V^{-1} s^{-1} were observed. Such mobilities are in agreement with mobility values reported from measurements along the *b*-axis of the perylene monoclinic unit cell.[44,48] As previously described for members of the acene family (e.g., pentacene electron mobility by inversion at RT is 0.5 cm^2 V^{-1} s^{-1}),[36] perylene is also ambipolar, having a hole mobility of 0.4 cm^2 V^{-1} s^{-1} at RT and 100 cm^2 V^{-1} s^{-1} at lower temperatures. A RT electron mobility of 5.5 cm^2 V^{-1} s^{-1} provides a new ceiling value to attain for novel n-type materials.

More recently, Sudhölter and co-workers reported on the liquid crystalline and charge transport properties of three *N,N′*-dialkylated, perylene diimides.[134] In particular, *N,N′*-dioctadecyl-3,4,9,10-perylenetetracarboxylic diimide (PTCDI-C18) demonstrated several crystalline and liquid crystalline phases, consistent with X-ray diffraction experiments that show a high degree of order in all three dimensions. X-ray experiments on the liquid crystal (LC) phases suggest smectic ordering, which is consistent with theoretical models, in which extensive interdigitation of the linear alkyl chains is assumed. Charge carrier mobilities were assessed by pulse-radiolysis time-resolved microwave conductivity and values >0.1 cm^2 V^{-1} s^{-1} were measured for LC phases and >0.2 cm^2 V^{-1} s^{-1} for crystalline phases.

We have recently shown that OTFTs based on *N,N′*-dioctyl-3,4,9,10-perylenetetracarboxylic diimide (PTCDI-C8) as the organic semiconductor provides bottom contact devices with mobilities as high as 0.6 cm^2 V^{-1} s^{-1} in the saturation regime and current on/off ratios $>10^5$.[61] High threshold voltages (ca. 75 V) were observed and are attributed to the formation of traps related to structural defects close to the metal contacts, in addition to band offsets.[117] X-ray studies in reflection mode revealed a (001) peak at ca. 20 Å, which is consistent with modeling studies that predict 21 Å, based on extensively interdigitated alkyl chains. This is consistent with the expected smectic ordering observed by Sudhölter (vide supra).

Although historically, metallophthalocyanines have been examined as p-type,[135] appropriate substitution can allow for the fine tuning of the HOMO–LUMO levels thus altering the majority charge carrier of the material.[136] For example, the work of Bao et al. explored a variety of metallophthalocyanines as channels in n-type OTFTs.[137] Chemical functionality, substrate temperature during the deposition as well as the metal center used were all critical to device performance. Optimum results were obtained with a perfluorinated phthalocyanine having M = Cu (F_{16}CuPc) and T_{dep} = 125 °C. It is interesting to note that the effect of fluorinating the rings results in a 1.6 eV drop in the LUMO level, as assessed by ultraviolet photoelectron spectroscopy (UPS) measurements and ultraviolet-visible (UV-vis) data, thus clearly indicating the advantageous effect of functionalizing materials with electron withdrawing groups for n-type applications. This approach presents an interesting design rule in which known p-type materials can be converted to n-type materials by simply lowering the LUMO levels via substitution with strong electron withdrawing groups. This is analogous to functionalizing naphthalene or perylene with electron withdrawing diimide moieties. A mobility of 3×10^{-2} cm^2 V^{-1} s^{-1} and on/off ratio in the range of 10^4–10^5 was obtained for F_{16}CuPc.[137] Furthermore, these devices could be stored in air for half a year and showed no decrease in mobility or on/off ratio. The edge on stacking of the molecules, effectively resulting in a fluorinated barrier at the surface, could be contributing to the unusual air stability observed in these devices, effectively providing a kinetic barrier as observed with NTCDI-C8F (vide supra).

More recently, Schön et al. studied the electron transport in single crystals of F_{16}CuPc in air as a function of time and temperature.[138] Space charge limited current (SCLC) spectroscopy was used to estimate the intrinsic mobility in single crystals. Charge transport was measured in the π-stacking direction for both single crystals and thin films, in order to eliminate the effect of transport anisotropy, while focusing on the effect of grain boundaries, disorder and other extrinsic parameters. Mobilities as high as 1.7 cm^2 V^{-1} s^{-1} at RT were estimated for the trap-free SCLC regime. At low temperatures (below 100–150 K) the effective mobility is dominated by trapping and thus it is thermally activated, whereas at higher temperatures, the effective mobility follows a power law dependence suggesting that band-like transport that is limited by phonon scat-

© WILEY-VCH Verlag GmbH, D-69469 Weinheim, 2002

tering is the dominant mechanism. This observation is analogous to what is observed with perylene single crystals.[47,48,132] This is in contrast to what is observed with thin films, in which thermally activated transport over a barrier related to grain boundaries is the dominant transport mechanism as described in a previous section. Studies on single crystals in air revealed that the mobility reaches stability after ca. 500 h. Annealing the crystals in the presence of hydrogen provides the original mobility. Thin films, prepared by thermal evaporation onto 125 °C substrates were also examined. The FET mobility is temperature independent at low temperature where tunneling becomes the dominant transport mechanism whereas it is thermally activated at higher temperatures. In conclusion, the intrinsic mobility is said to be band-like in a wide temperature range due to the temperature dependence of the mobility for single crystals, whereas polycrystalline films have their charge transport dominated by grain boundary effects.

Recently, Facchetti et al. reported on the use of α,ω-diperfluorohexylsexithiophene (DHF-6T) as a novel n-type organic semiconductor.[139] Once again, a known p-type material (i.e., DH6T) was converted to n-type by simply functionalizing it with appropriate electron withdrawing groups. Although the HOMO–LUMO gap remains the same for both DHF-6T and DH6T (ca. 2.4 eV), redox studies reveal an anodic shift of ca. +0.27 V, thus significantly increasing the ionization potential of DHF-6T and providing a LUMO level ca. 0.27 V below that of DH6T. This result is analogous to what was described for F_{16}CuPc (vide supra). Elevated substrate temperatures were shown to produce grains with larger dimensions and the use of a surface pretreated with 1-(trichlorosilyl)-1,1,2,2-tetrahydroperfluorooctane (TPFO) led to ca. 10 % increase in crystallite size. More importantly grain–grain and grain–substrate gaps were considerably smaller. Top contact devices were prepared by pre-treating SiO_2 surfaces with either HMDS or TPFO prior to the deposition of DHF-6T due to the hydrophilic nature of the oxide. Under a nitrogen atmosphere, mobilities of 0.02 $cm^2\,V^{-1}\,s^{-1}$ and a current on/off ratio of 10^5 were obtained in the saturation regime using gold electrodes. Similar results were obtained with aluminum electrodes. Air stability was not addressed. These devices were obtained via depositions where the substrate temperature was 80–100 °C. Alternatively, mobilities of 10^{-4} were obtained when the temperature was ca. 50 °C or 120 °C. It is interesting to note that the turn-on voltage increases with time, thus resulting in a decrease in on current, yet the turn-on voltage can be stabilized and reduced by post film growth annealing.

In summary, great progress has been achieved with n-type OTFTs over the last 10 years. Mobilities ranging from 0.001–0.6 $cm^2\,V^{-1}\,s^{-1}$ and current on/off ratio $>10^5$ have been achieved and in some cases air stable devices have been realized.

9. Conclusions

There has been tremendous progress in OTFT performance during the last decade. Our understanding of the properties and OTFT device operation has improved dramatically. Advances in device performance characteristics have resulted from the introduction of novel materials either obtained by chemical modification of existing ones or by the synthesis of completely new structures, followed by optimization of their morphology and structural order.

At present, we have reached the point at which an initial product application can be seriously considered. Organic semiconductors, such as pentacene, deposited by vacuum-sublimation remain the best performers due to not only their molecular electronic properties but also their very well ordered films, which result from the use of this highly controllable deposition method. However, substantial improvements have taken place in solution-processed organic semiconductors too, and their mobilities are currently only one order of magnitude lower than those of vapor-deposited pentacene TFTs. There is a potentially important cost-advantage associated with the solution processing of organic TFTs, as it eliminates the need for expensive vacuum chambers and lengthy pump-down cycles. However, for this advantage to be realized, all or at least most of the layers comprising the TFT device should be deposited using methods that do not involve vacuum deposition. These layers include the source, drain, and gate electrodes that currently are made of high work function metals, the gate dielectric, and the (potentially necessary for some materials) passivation/encapsulation layer. Reel-to-reel processing, which has obvious advantages over batch fabrication processes for reducing costs, can be applied to both vacuum- and solution-deposited organic semiconductors; thus it does not constitute an exclusive advantage for either of the two classes of materials. If, however, one takes into account the ability to stamp or print solution based organics, thus eliminating traditional lithographic steps, then their potential cost advantage over vacuum deposited organics is apparent. Good device stability and long lifetimes are also required in order to fully realize the benefits of organic electronics. The future looks promising for inexpensive organic electronics as new and improved materials with unique electronic properties are being introduced and integrated into functional devices.

Received: August 10, 2001
Final version: October 31, 2001

[1] M. Pope, C. E. Swenberg, *Electronic Processes in Organic Crystals and Polymers*, 2nd ed., Oxford University Press, Oxford **1999**, pp. 337–340.
[2] C. W. Tang, S. A. Van Slyke, *Appl. Phys. Lett.* **1987**, *51*, 913.
[3] J. H. Burroughes, D. D. Bradley, A. R. Brown, R. N. Marks, K. Mackay, R. H. Friend, P. L. Burn, A. B. Holmes, *Nature* **1990**, *347*, 539.
[4] F. Ebisawa, T. Kurokawa, S. Nara, *J. Appl. Phys.* **1983**, *54*, 3255.
[5] K. Kudo, M. Yamashina, T. Moriizumi, *Jpn. J. Appl. Phys* **1984**, *23*, 130.
[6] A. Tsumura, H. Koezuka, T. Ando, *Appl. Phys. Lett.* **1986**, *49*, 1210.
[7] For previously published graphs of device performance vs. year reported see: a) C. D. Dimitrakopoulos, B. K. Furman, T. Graham, S. Hegde, S. Purushothaman, *Synth. Met.* **1998**, *92*, 47. b) A. Hellemans, *Science* **1999**, *283*, 771.
[8] R. H. Friend, J. Burroughes, T. Shimoda, *Phys. World* **1999**, *12*, 35.
[9] S. Forrest, *MRS Bull.* **2001**, *February*, 108.
[10] G. Yu, A. J. Heeger, in *Proceedings of 23rd International Conference on the Physics of Semiconductors*, Vol. 1 (Eds: M. Scheffler, R. Zimmerman), World Scientific, Singapore **1996**, p. 35.

 © WILEY-VCH Verlag GmbH, D-69469 Weinheim, 2002 0935-9648/02/0201-0115 $ 17.50+.50/0

[11] P. Ostoja, S. Guerri, S. Rossini, M. Servidori, C. Taliani, R. Zamboni, *Synth. Met.* **1993**, *54*, 447.
[12] A. Dodabalapur, L. Torsi, H. E. Katz, *Science* **1995**, *268*, 270.
[13] N. Greenham, R. H. Friend, in *Solid State Physics; Advances in Research and Applications*, Vol. 49 (Eds: H. Ehrenreich, F. Spaepen), Academic, San Diego, CA **1995**, pp. 1–149.
[14] A. J. Lovinger, L. J. Rothberg, *J. Mater. Res.* **1996**, *11*, 1581.
[15] H. E. Katz, *J. Mater. Chem.* **1997**, *7*, 369.
[16] A. R. Brown, C. P. Jarrett, D. M. de Leeuw, M. Matters, *Synth. Met.* **1997**, *88*, 37.
[17] F. Garnier, *Chem. Phys.* **1998**, *227*, 253.
[18] G. Horowitz, *Adv. Mater.* **1998**, *10*, 3.
[19] H. E. Katz, Z. Bao, *J. Phys. Chem. B* **2000**, *104*, 671.
[20] *Carbon Nanotubes: Synthesis, Structure, Properties, and Applications* (Eds: M. Dresselhaus, G. Dresselhaus, P. Avouris), Springer, Berlin **2001**.
[21] C. Joachim, J. K. Gimzewski, A. Aviram, *Nature* **2000**, *408*, 541.
[22] C. Dekker, *Phys. Today* **1999**, *52*, 22.
[23] J. M. Tour, *Acc. Chem. Res.* **2000**, *33*, 791.
[24] a) P. G. Collins, M. R. Arnold, P. Avouris, *Science* **2001**, *292*, 706. b) R. Martel, T. Schmidt, H. R. Shea, T. Hertel, P. Avouris, *Appl. Phys. Lett.* **1998**, *73*, 2447.
[25] Y. Taur, T. H. Ning, *Fundamentals of Modern VLSI Devices*, Cambridge University Press, Cambridge **1998**, p. 11.
[26] R. Wisnieff, *Nature* **1998**, *394*, 225.
[27] B. Comiskey, J. D. Albert, H. Yoshizawa, J. Jacobson, *Nature* **1998**, *394*, 253.
[28] N. K. Sheridon, *US Patent 4 126 854*, **1978**.
[29] B. Crone, A. Dodabalapur, A. Gelperin, L. Torsi, H. E. Katz, A. J. Lovinger, Z. Bao, *Appl. Phys. Lett.* **2001**, *78*, 2229.
[30] C. J. Drury, C. M. J. Mutsaers, C. M. Hart, M. Matters, D. M. de Leeuw, *Appl. Phys. Lett.* **1998**, *73*, 108.
[31] J. H. Schön, C. Kloc, B. Batlogg, *Org. Electron.* **2000**, *1*, 57.
[32] P. E. Burrows, S. R. Forrest, L. S. Sapochak, J. Schwartz, P. Fenter, T. Buma, V. S. Ban, J. L. Forrest, *J. Cryst. Growth* **1995**, *156*, 91.
[33] M. Baldo, M. Deutsch, P. Burrows, H. Gossenberger, M. Gerstenberg, V. Ban, S. Forrest, *Adv. Mater.* **1998**, *10*, 1505.
[34] C. Kloc, P. G. Simpkins, T. Siegrist, R. A. Laudise, *J. Cryst. Growth* **1997**, *182*, 416.
[35] R. A. Laudise, C. Kloc, P. G. Simpkins, T. Siegrist, *J. Cryst. Growth* **1998**, *187*, 449.
[36] J. H. Schön, S. Berg, C. Kloc, B. Batlogg, *Science* **2000**, *287*, 1022.
[37] S. F. Nelson, Y.-Y. Lin, D. J. Gundlach, T. N. Jackson, *Appl. Phys. Lett.* **1998**, *72*, 1854.
[38] Y.-Y. Lin, D. J. Gundlach, S. Nelson, T. N. Jackson, *IEEE Electron Device Lett.* **1997**, *18*, 606.
[39] C. Dimitrakopoulos, S. Purushothaman, J. Kymissis, A. Callegari, J. M. Shaw, *Science* **1999**, *283*, 822.
[40] W. Warta, R. Stehle, N. Karl, *Appl. Phys. A* **1985**, *36*, 163.
[41] N. Karl, J. Marktanner, R. Stehle, W. Warta, *Synth. Met.* **1991**, *41–43*, 2473.
[42] J. H. Schön, C. Kloc, B. Batlogg, *Science* **2000**, *288*, 2338.
[43] J. H. Schön, B. Batlogg, *J. Appl. Phys.* **2001**, *89*, 336.
[44] N. Karl, *Organic Electronic Materials*, Part II (Eds: R. Farchioni, G. Grosso), Springer, Berlin **2001**, Ch. 8.
[45] D. M. Burland, *Phys. Rev. Lett.* **1974**, *33*, 833.
[46] D. M. Burland, U. Konzelmann, *J. Chem. Phys.* **1977**, *67*, 319.
[47] E. A. Silinsh, V. Cğápek, *Organic Molecular Crystals: Interaction Localization and Transport Phenomena*, AIP, New York **1994**, Ch. 7.
[48] N. Karl, in *Landolt-Börnstein, Group III, Semiconductors, Organic Semiconductors*, Vol. 17 (Ed: O. Madelung), Springer, Berlin **1985**, pp. 106–218.
[49] S. M. Sze, *Physics of Semiconductor Devices*, 2nd ed., Wiley, New York **1981**, pp. 438–453.
[50] C. D. Dimitrakopoulos, A. R. Brown, A. Pomp, *J. Appl. Phys.* **1996**, *80*, 2501.
[51] G. Horowitz, R. Hajlaoui, R. Bourgouiga, M. Hajlaoui, *Synth. Met.* **1999**, *101*, 401.
[52] L. Torsi, A. Dodabalapur, H. E. Katz, *J. Appl. Phys.* **1995**, *78*, 1088.
[53] L. Kosbar, C. D. Dimitrakopoulos, D. J. Mascaro, *Mater. Res. Soc. Symp. Proc.* **2001**, *665*.
[54] C. D. Dimitrakopoulos, L. Kosbar, unpublished results.
[55] Y.-Y. Lin, D. J. Gundlach, S. Nelson, T. N. Jackson, *IEEE Trans. Electron Devices* **1997**, *44*, 1325.
[56] C. D. Dimitrakopoulos, unpublished results. This relatively high voltage measurement was performed on a Keithley 4200 SCS.
[57] G. Horowitz, M. E. Hajlaoui, R. Hajlaoui, *J. Appl. Phys.* **2000**, *87*, 4456.
[58] G. Horowitz, M. E. Hajlaoui, *Adv. Mater.* **2000**, *12*, 1046.
[59] Y.-Y. Lin, D. J. Gundlach, T. N. Jackson, *54th Annual Device Research Conference Digest* **1996**, p. 80.
[60] D. J. Gundlach, personal communication.
[61] P. R. L. Malenfant, C. D. Dimitrakopoulos, J. D. Gelorme, L. L Kosbar, T. O. Graham, A. Curioni, W. Andreoni, unpublished.
[62] T. Jentzsch, H. J. Juepner, K. W. Brzezinka, A. Lau, *Thin Solid Films* **1998**, *315*, 273.
[63] T. Minakata, H. Imai, M. Ozaki, *J. Appl. Phys.* **1992**, *72*, 4178.
[64] T. Minakata, M. Ozaki, H. Imai, *J. Appl. Phys.* **1993**, *74*, 1079.
[65] G. Horowitz, D. Fichou, X. Peng, Z. Xu, F. Garnier, *Solid State Commun.* **1989**, *72*, 381.
[66] G. Horowitz, X. Peng, D. Fichou, F. Garnier, *Synth. Met.* **1992**, *51*, 419.
[67] F. Garnier, A. Yassar, R. Hajlaoui, G. Horowitz, F. Dellofre, B. Servet, S. Ries, P. Alnot, *J. Am. Chem. Soc.* **1993**, *115*, 8716.
[68] C. D. Dimitrakopoulos, D. J. Mascaro, *IBM J. Res. Dev.* **2001**, *45*, 11.
[69] R. B. Campbell, J. Monteath Robertson, J. Trotter, *Acta Cryst.* **1961**, *14*, 705.
[70] F. J. Meyer zu Heringdorf, M. C. Reuter, R. M. Tromp, *Nature* **2001**, *412*, 517.
[71] C. D. Dimitrakopoulos, J. Kymissis, S. Purushothaman, D. A. Neumayer, P. R. Duncombe, R. B. Laibowitz, *Adv. Mater.* **1999**, *11*, 1372.
[72] D. J. Gundlach, H. Klauk, C. D. Sheraw, C.-C. Kuo, J.-R. Huang, T. N. Jackson, *International Electron Devices Meeting Technical Digest* **1999**, pp. 111–114.
[73] C. P. Jarret, A. R. Brown, R. H. Friend, M. G. Harrison, D. M. de Leeuw, P. Herwig, K. Mullen, *Synth. Met.* **1997**, *85*, 1403.
[74] P. G. Le Comber, W. E. Spear, *Phys. Rev. Lett.* **1970**, *25*, 509.
[75] G. Horowitz, R. Hajlaoui, P. Delannoy, *J. Phys. III* **1995**, *5*, 355.
[76] G. Horowitz, R. Hajlaoui, D. Fichou, A. El Kassmi, *J. Appl. Phys.* **1999**, *85*, 3202.
[77] I. Muzicante, E. A. Silinsh, *Acta Phys. Pol. A* **1995**, *88*, 389.
[78] J. H. Schön, C. Kloc, *Appl. Phys. Lett.* **2001**, *78*, 3821.
[79] A. B. Chwang, C. D. Frisbie, *J. Appl. Phys.* **2001**, *90*, 1342.
[80] M. C. J. M. Vissenberg, M. Matters, *Phys. Rev. B* **1998**, *57*, 12 964.
[81] Z. G. Yu, D. L. Smith, A. Saxena, R. L. Martin, A. R. Bishop, *Phys. Rev. Lett.* **2000**, *84*, 721.
[82] C. D. Dimitrakopoulos, J. Kymissis, S. Purushothaman, in *Proceedings of The Int. Conf. on Digital Printing Technologies*, NIP16, Society of Imaging Science and Technology, Vancouver **2000**, pp. 493–496.
[83] J. Kymissis, *M.S. Thesis*, Mass. Inst. Tech., Cambridge, MA **1999**.
[84] J. Kymissis, C. D. Dimitrakopoulos, S. Purushothaman, *IEEE Trans. Electron Devices* **2001**, *48*, 1060. See also: Correction to this paper, *IEEE Trans. Electron Devices* **2001**, *48*, 1750.
[85] A. Assadi, C. Svensson, M. Willander, O. Inganäs, *Appl. Phys. Lett.* **1988**, *53*, 195.
[86] A. Tsumura, H. Fuchigami, H. Koezuka, *Synth. Met.* **1991**, *41*, 1181.
[87] J. Paloheimo, H. Stubb, P. Yli-Lahti, P. Kuivalainen, *Synth. Met.* **1991**, *41–43*, 563.
[88] R. D. McCullough, *Adv. Mater.* **1998**, *10*, 93. R. D. McCullough, R. D. Lowe, *J. Chem. Soc., Chem. Commun.* **1992**, 70. T.-A. Chen, R. D. Rieke, *J. Am. Chem. Soc.* **1992**, *114*, 10 087. T.-A. Chen, X. Wu, R. D. Rieke, *J. Am. Chem. Soc.* **1995**, *117*, 233.
[89] Z. Bao, A. Dodabalapur, A. J. Lovinger, *Appl. Phys. Lett.* **1996**, *69*, 4108.
[90] H. Sirringhaus, P. J. Brown, R. H. Friend, M. M. Nielsen, K. Bechgaard, B. M. W. Langeveld-Voss, A. J. H. Spiering, R. A. J. Janssen, E. W. Meijer, P. T. Herwig, D. M. de Leeuw, *Nature* **1999**, *401*, 685.
[91] H. Sirringhaus, N. Tessler, R. H. Friend, *Science* **1998**, *280*, 1741.
[92] H. Sirringhaus, N. Tessler, R. H. Friend, *Synth. Met.* **1999**, *102*, 857.
[93] Z. Bao, Y. Feng, A. Dodabalapur, V. R. Raju, A. J. Lovinger, *Chem. Mater.* **1997**, *9*, 1299.
[94] J. H. Schön, A. Dodabalapur, Z. Bao, C. Kloc, O. Schenker, B. Batlogg, *Nature* **2001**, *410*, 189.
[95] R. L. Greene, G. B. Street, L. J. Suter, *Phys. Rev. Lett.* **1975**, *34*, 577.
[96] K. Bechgaard, D. Jérome, *Sci. Am.* **1982**, *247*, 52. D. Jérome, K. Bechgaard, *Nature* **2001**, *410*, 162.
[97] H. Sirringhaus, T. Kawase, R. H. Friend, T. Shimoda, M. Inbasekaran, W. Wu, E. P. Woo, *Nature* **2000**, *290*, 2123.
[98] H. Sirringhaus, R. J. Wilson, R. H. Friend, M. Inbasekaran, W. Wu, E. P. Woo, M. Grell, D. D. C. Bradley, *Appl. Phys. Lett.* **2000**, *77*, 406.
[99] J. Paloheimo, P. Kuivalainen, H. Stubb, E. Vuorimaa, P. Yli-Lahti, *Appl. Phys. Lett.* **1990**, *56*, 1157.
[100] J. Paloheimo, H. Stubb, P. Yli-Lahti, P. Dyreklev, O. Inganäs, *Thin Solid Films* **1992**, *210/211*, 283.
[101] G. Xu, Z. Bao, J. T. Groves, *Langmuir* **2000**, *16*, 1834.
[102] T. Bjørnholm, D. R. Greve, N. Reitzel, T. Hassenkam, K. Kjaer, P. B. Howes, N. B. Larsen, J. Bøgelund, M. Jayaraman, P. C. Ewbank, R. D. McCullough, *J. Am. Chem. Soc.* **1998**, *120*, 7643.
[103] H. Akimichi, K. Waragai, S. Hotta, H. Kano, H. Sakaki, *Appl. Phys. Lett.* **1991**, *58*, 1500.

 © WILEY-VCH Verlag GmbH, D-69469 Weinheim, 2002 0935-9648/02/0201-0116 $ 17.50+.50/0

[104] H. E. Katz, A. J. Lovinger, J. Johnson, C. Kloc, T. Siegrist, W. Li, Y.-Y. Lin, A. Dodabalapur, *Nature* **2000**, *404*, 478.
[105] H. E. Katz, J. G. Laquindanum, A. J. Lovinger, *Chem. Mater.* **1998**, *10*, 633.
[106] H. E. Katz, W. Li, A. J. Lovinger, J. G. Laquindanum, *Synth. Met.* **1999**, *102*, 897.
[107] F. Garnier, R. Hajlaoui, A. E. Kassmi, G. Horowitz, L. Laigre, W. Porzio, M. Armanini F. Provasoli, *Chem. Mater.* **1998**, *10*, 3334.
[108] J. G. Laquindanum, H. E. Katz, A. J. Lovinger, *J. Am. Chem. Soc.* **1998**, *120*, 664.
[109] C. D. Dimitrakopoulos, A. Afzali-Ardakani, B. Furman, J. Kymissis, S. Purushothaman, *Synth. Met.* **1997**, *89*, 193.
[110] A. R. Brown, A. Pomp, D. M. deLeeuw, D. B. M. Klaassen, E. E. Havinga, P. T. Herwig, K. Müllen, *J. Appl. Phys.* **1996**, *79*, 2136.
[111] A. R. Brown, A. Pomp, C. M. Hart, D. M. de Leeuw, *Science* **1995**, *270*, 972.
[112] P. T. Herwig, K. Müllen, *Adv. Mater.* **1999**, *11*, 480.
[113] J. H. Burroughes, C. A. Jones, R. H. Friend, *Nature* **1988**, *335*, 137.
[114] J. H. Burroughes, R. H. Friend, P. C. Allen, *J. Phys. D: Appl. Phys.* **1989**, *22*, 956.
[115] D. M. de Leeuw, M. M. J. Simenon, A. R. Brown, R. E. F. Einerhand, *Synth. Met.* **1997**, *87*, 53.
[116] Tabulated redox data obtained in aqueous media are not always representative of redox processes occurring in the bulk.
[117] I. H. Campbell, J. D. Kress, R. L. Martin, D. L. Smith, N. N. Barashkov, J. P. Ferraris, *Appl. Phys. Lett.* **1997**, *71*, 3528.
[118] H. Ishii, K. Seki, *IEEE Trans. Electron Devices* **1997**, *44*, 1295. I. G. Hill, A. Rajagopal, A. Kahn, *Appl. Phys. Lett.* **1998**, *73*, 662.
[119] G. Guillaud, M. Al Sadound, M. Maitrot, *Chem. Phys. Lett.* **1990**, *167*, 503.
[120] A. R. Brown, D. M. de Leeuw, E. J. Lous, E. E. Havinga, *Synth. Met.* **1994**, *66*, 257.
[121] R. C. Haddon, A. S. Perel, R. C. Morris, T. T. M. Palstra, A. F. Hebard, R. M. Fleming, *Appl. Phys. Lett.* **1995**, *67*, 121.
[122] P.-M. Allemand, K. C. Khemani, A. Koch, F. Wudl, K. Holczer, S. Donovan, G. Grüner, J. D. Thompson, *Science* **1991**, *253*, 301.
[123] E. Frankevich, Y. Maruyama, H. Ogata, *Chem. Phys. Lett.* **1993**, *214*, 39.
[124] J. G. Laquindanum, H. E. Katz, A. Dodabalapur, A. J. Lovinger, *J. Am. Chem. Soc.* **1996**, *118*, 11 331.
[125] H. E. Katz, J. Johnson, A. J. Lovinger, W. Li, *J. Am. Chem. Soc.* **2000**, *122*, 7787.
[126] H. E. Katz, T. Siegrist, J. H. Schön, C. Kloc, B. Batlogg, A. J. Lovinger, J. Johnson, *Chem. Phys. Chem.* **2001**, 167.
[127] G. Horowitz, F. Kouki, P. Spearman, D. Fichou, C. Nogues, X. Pan, F. Garnier, *Adv. Mater.* **1996**, *8*, 242.
[128] J. R. Ostrick, A. Dodabalapur, L. Torsi, A. J. Lovinger, E. W. Kwock, T. M. Miller, M. Galvin, M. Berggren, H. E. Katz, *J. Appl. Phys.* **1997**, *81*, 6804. See also: D. Y. Zang, F. So, S. R. Forrest, *Appl. Phys. Lett.* **1991**, *59*, 823.
[129] S. R. Forrest, M. L. Kaplan, P. H. Schmidt, *J. Appl. Phys.* **1984**, *55*, 1492. S. R. Forrest, M. L. Kaplan, P. H. Schmidt, *J. Appl. Phys.* **1984**, *56*, 543.
[130] P. E. Fenter, P. E. Burrows, P. Eisenberger, S. R. Forrest, *J. Cryst. Growth* **1995**, *152*, 65.
[131] N. Karl, J. Marktanner, *Mol. Cryst. Liq. Cryst.* **1998**, *315*, 163.
[132] N. Karl, K.-H. Kraft, J. Marktanner, M. Münch, F. Schatz, R. Stehle, H.-M. Uhde, *J. Vac. Sci. Technol. A* **1999**, *17*, 2318.
[133] J. H. Schön, C. Kloc, B. Batlogg, *Appl. Phys. Lett.* **2000**, *77*, 3776.
[134] C. W. Struijk, A. B. Sieval, J. E. J. Dakhorst, M. van Dijk, P. Kimkes, R. B. M. Koehorst, H. Donker, T. J. Schaafsma, S. J. Picken, A. M. van de Craats, J. M. Warman, H. Zuilhof, E. J. R. Sudhölter, *J. Am. Chem. Soc.* **2000**, *122*, 11 057.
[135] a) Z. Bao, A. J. Lovinger, A. Dodabalapur, *Appl. Phys. Lett.* **1996**, *69*, 3066. b) Z. Bao, A. J. Lovinger, A. Dodabalapur, *Adv. Mater.* **1997**, *9*, 42. c) G. Guillaud, J. Simon, *Chem. Phys. Lett.* **1994**, *219*, 123. d) G. Guillaud, R. B. Chaabane, C. Jouve, M. Gamoudi, *Thin Solid Films* **1995**, *258*, 279.
[136] E. Karmann, J.-P. Meyer, D. Schlettwein, N. I. Jaeger, M. Anderson, A. Schmidt, N. R. Armstrong, *Mol. Cryst. Liq. Cryst.* **1996**, *283*, 283.
[137] Z. Bao, A. J. Lovinger, J. Brown, *J. Am. Chem. Soc.* **1998**, *120*, 207.
[138] J. H. Schön, C. Kloc, Z. Bao, B. Batlogg, *Adv. Mater.* **2000**, *12*, 1539. J. H. Schön, Z. Bao, *J. Appl. Phys.* **2001**, *89*, 3526.
[139] A. Facchetti, Y. Deng, A. Wang, Y. Koide, H. Sirringhaus, T. J. Marks, R. H. Friend, *Angew. Chem. Int. Ed.* **2000**, *39*, 4547.
[140] G. H. Heilmeier, L. A. Zanoni, *J. Phys. Chem. Solids* **1964**, *25*, 603.
[141] C. Clarisse, M. T. Riou, M. Gauneau, M. Le Contellec, *Electron. Lett.* **1988**, *24*, 674.
[142] J. Paloheimo, E. Punkka, H. Stubb, P. Kuivalainen, in *Lower Dimensional Systems and Molecular Devices*, Proceedings of NATO ASI, Spetses, Greece (Ed: R. M. Mertzger), Plenum, New York **1989**.
[143] H. Fuchigami, A. Tsumura, H. Koezuka, *Appl. Phys. Lett.* **1993**, *63*, 1372.
[144] F. Garnier, R. Hajlaoui, A. Yassar, P. Srivastava, *Science* **1994**, *265*, 1684.
[145] Z. Bao, A. J. Lovinger, A. Dodabalapur, *Appl. Phys. Lett.* **1996**, *69*, 3066.
[146] H. Sirringhaus, R. H. Friend, X. C. Li, S. C. Moratti, A. B. Holmes, N. Feeder, *Appl. Phys. Lett.* **1997**, *71*, 3871.
[147] H. E. Katz, A. J. Lovinger, J. G. Laquindanum, *Chem. Mater.* **1998**, *10*, 457.
[148] J. Kastner, J. Paloheimo, H. Kuzmany, in *Solid State Sciences* (Eds: H. Kuzmany, M. Mehring, J. Fink), Springer, New York **1993**, pp. 521–515.

 © WILEY-VCH Verlag GmbH, D-69469 Weinheim, 2002 0935-9648/02/0201-0117 $ 17.50+.50/0